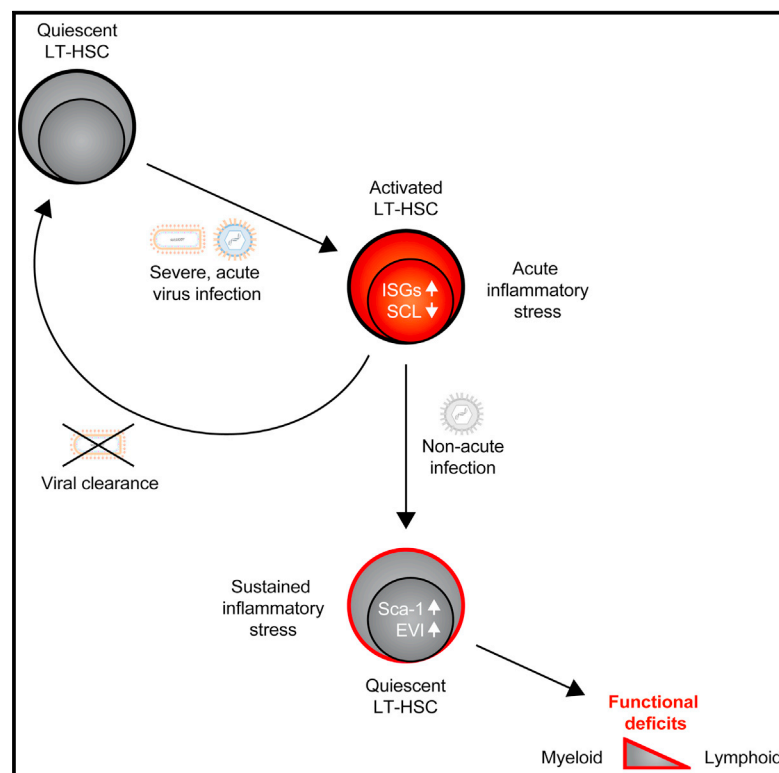


Cell Reports

Systemic Virus Infections Differentially Modulate Cell Cycle State and Functionality of Long-Term Hematopoietic Stem Cells In Vivo

Graphical Abstract



Authors

Christoph Hirche, Theresa Frenz, Simon F. Haas, ..., Andreas Trumpp, Marieke A.G. Essers, Ulrich Kalinke

Correspondence

ulrich.kalinke@twincore.de

In Brief

Long-term hematopoietic stem cells (LT-HSCs) are activated by recombinant type I interferon (IFN-I). Hirche et al. report here that acute systemic virus infections activate LT-HSCs independently of IFN-I receptor signaling. Non-acute infection of bone marrow donors impacts LT-HSC function, but not phenotype, potentially explaining clinical complications following bone marrow transplantations.

Highlights

- Acute virus infections activate LT-HSCs independently of IFN-I receptor signaling
- A bone marrow-intrinsic inflammatory threshold prevents excessive LT-HSC activation
- Non-acute MCMV infection alters the bone marrow milieu and LT-HSC gene expression
- Despite the return to phenotypic quiescence, LT-HSCs retain functional deficits



Systemic Virus Infections Differentially Modulate Cell Cycle State and Functionality of Long-Term Hematopoietic Stem Cells In Vivo

Christoph Hirche,^{1,10,11} Theresa Frenz,^{1,10} Simon F. Haas,^{2,3,10} Marius Döring,¹ Katharina Borst,¹ Pia-K. Tegtmeyer,¹ Ilija Brizic,⁴ Stefan Jordan,⁵ Kirsten Keyser,⁶ Chintan Chhatbar,¹ Eline Pronk,^{2,3} Shuiping Lin,⁷ Martin Messerle,⁶ Stipan Jonjic,⁴ Christine S. Falk,⁸ Andreas Trumpp,^{2,9} Marieke A.G. Essers,^{2,3} and Ulrich Kalinke^{1,12,*}

¹Institute for Experimental Infection Research, TWINCORE, Centre for Experimental and Clinical Infection Research, a joint venture between the Hannover Medical School and the Helmholtz Centre for Infection Research, 30625 Hannover, Germany

²Heidelberg Institute for Stem Cell Technology and Experimental Medicine (HI-STEM gGmbH), 69120 Heidelberg, Germany

³"Hematopoietic Stem Cells and Stress" Group, German Cancer Research Centre (DKFZ), 69121 Heidelberg, Germany

⁴Department of Histology and Embryology, Faculty of Medicine, University of Rijeka, 51000 Rijeka, Croatia

⁵Icahn School of Medicine at Mount Sinai, Department of Oncological Sciences, New York, NY 10029, USA

⁶Department of Virology, Hannover Medical School, 30625 Hannover, Germany

⁷Molecular Medicine Division, Walter and Eliza Hall Institute of Medical Research, Parkville, VIC 3052, Australia

⁸Institute of Transplant Immunology, IFB-Tx, Hannover Medical School, 30625 Hannover, Germany

⁹Division of Stem Cells and Cancer, German Cancer Research Centre (DKFZ), 69120 Heidelberg, Germany

¹⁰These authors contributed equally

¹¹Present address: Heidelberg Institute for Stem Cell Technology and Experimental Medicine (HI-STEM gGmbH), 69120 Heidelberg, Germany

¹²Lead Contact

*Correspondence: ulrich.kalinke@twincore.de
<http://dx.doi.org/10.1016/j.celrep.2017.05.063>

SUMMARY

Quiescent long-term hematopoietic stem cells (LT-HSCs) are efficiently activated by type I interferon (IFN-I). However, this effect remains poorly investigated in the context of IFN-I-inducing virus infections. Here we report that both vesicular stomatitis virus (VSV) and murine cytomegalovirus (MCMV) infection induce LT-HSC activation that substantially differs from the effects triggered upon injection of synthetic IFN-I-inducing agents. In both infections, inflammatory responses had to exceed local thresholds within the bone marrow to confer LT-HSC cell cycle entry, and IFN-I receptor triggering was not critical for this activation. After resolution of acute MCMV infection, LT-HSCs returned to phenotypic quiescence. However, non-acute MCMV infection induced a sustained inflammatory milieu within the bone marrow that was associated with long-lasting impairment of LT-HSC function. In conclusion, our results show that systemic virus infections fundamentally affect LT-HSCs and that also non-acute inflammatory stimuli in bone marrow donors can affect the reconstitution potential of bone marrow transplants.

INTRODUCTION

A scarce population of long-term hematopoietic stem cells (LT-HSCs) is responsible for lifelong blood and immune cell genera-

tion (Morrison and Weissman, 1994). LT-HSCs reside in defined spatial and microenvironmental bone marrow niches (Morrison and Scadden, 2014), and they maintain a predominantly quiescent cell cycle state (Wilson et al., 2007). However, upon hematopoietic stress, such as blood loss, chemotherapy, anemia, or bone marrow aplasia, LT-HSC activation ensures efficient replenishment of blood and immune cells (Wilson et al., 2008).

Recently, inflammatory responses induced by Toll-like receptor (TLR) ligands (Nagai et al., 2006; Takizawa et al., 2011), most notably the synthetic RNA polyinosinic:polycytidylic acid (poly(I:C)) (Essers et al., 2009; Haas et al., 2015), were shown to induce cell cycle activation and differentiation of LT-HSCs. Poly(I:C) is a potent inducer of a type I interferon (IFN-I)-biased inflammatory response. IFN-I is triggered early upon virus infection and plays a pivotal role in establishing an anti-viral state and promoting immune cell-mediated virus clearance (Crouse et al., 2015). Importantly, the poly(I:C)-mediated cell cycle induction of LT-HSCs was shown to be mainly driven in an IFN-I receptor (IFNAR)- and STAT1-dependent manner (Essers et al., 2009). After poly(I:C)-mediated activation, LT-HSCs return to quiescence and, thus, avoid apoptosis and DNA damage (Pietras et al., 2014; Walter et al., 2015). Similar to IFN-I, also IFN-II (IFN- γ) has been linked to HSC activation (Baldridge et al., 2010), and particularly it triggers the differentiation of myeloid HSCs (Matatall et al., 2014).

Collectively, studies suggest that IFN-I induced upon injection of synthetic TLR ligands or injected as recombinant cytokine triggers LT-HSC cell cycle activation. Although of fundamental clinical importance, the effects of live, IFN-I-inducing viruses on LT-HSCs have not been intensively studied. Especially immunosuppressed bone marrow transplant patients are at enhanced



risk of severe infections with opportunistic pathogens, such as the obligatory human-specific β -herpesvirus cytomegalovirus (HCMV). In immunocompetent individuals primary HCMV infection is usually asymptomatic. However, in immunocompromised patients, the virus causes severe disease (Boeckh and Nichols, 2004), and acute HCMV viremia can even elicit graft rejection in bone marrow-transplanted patients (Fries et al., 2005).

Here we studied whether acute or non-acute virus infections induce inflammatory responses that would confer LT-HSC activation and affect their reconstitution potential. Our results indicate that peripheral virus infections induce inflammatory responses in blood and bone marrow that are capable of mediating LT-HSC cell cycle entry. Notably, this LT-HSC activation occurs largely independent of IFNAR signaling. Moreover, we show that acute virus infection impairs the reconstitution potential of LT-HSCs and that, even after resolution of acute virus infection and return to phenotypical quiescence, LT-HSCs continue to show a reduced reconstitution potential. Thus, our results establish a link between non-acute systemic infections of bone marrow donors and complications in transplant recipients.

RESULTS

High-Dose Virus Challenge or Uncontrolled Viral Replication Is Required for VSV-Induced Cell Cycle Activation of LT-HSCs

To investigate the impact of virus-induced IFN-I on LT-HSCs, wild-type (WT) and IFN-I receptor-deficient mice (IFNAR^{-/-}) were infected with vesicular stomatitis virus M2 (VSV). This virus lacks the immunomodulatory function of the M encoding gene (Stojdl et al., 2003), and, hence, it induces particularly strong IFN-I responses (Waibler et al., 2007). To analyze LKCD150⁺CD48⁺CD34⁺ LT-HSCs, lineage⁻c-Kit⁺ (LK) bone marrow was stained for signaling lymphocyte activation markers (SLAMFs) (Kiel et al., 2005) and CD34 (Osawa et al., 1996) (see Figure S1A and Haas et al., 2015 for fluorescence-activated cell sorting [FACS] gating strategy). Cell cycle status was determined 1 day post-infection (dpi) by Ki-67/Hoechst staining. As reported previously, treatment of WT mice with the synthetic RNA poly(I:C) resulted in cell cycle activation (G₁-S-G₂-M) of quiescent (G₀) LT-HSCs. Furthermore, LT-HSC activation was significantly reduced in IFNAR^{-/-} mice, indicating that poly(I:C)-induced IFN-I responses were critical (Figure 1A; Essers et al., 2009).

To investigate whether systemic infection with live viruses would also trigger IFNAR-dependent activation of LT-HSCs, we infected mice with 1×10^5 plaque-forming units (PFUs) VSV (VSV int). Surprisingly, this dose did not trigger LT-HSC cell cycle activation in WT but in IFNAR^{-/-} mice (Figure 1A). Of note, quantification of peripheral virus loads revealed that, unlike in immunocompetent WT mice, IFNAR^{-/-} mice showed uncontrolled virus replication and LT-HSC activation (Figure 1B). In both WT and IFNAR^{-/-} mice, VSV infection induced leukopenia 1 dpi (Figure S1B). However, while WT mice recovered by 2 dpi, IFNAR^{-/-} mice rapidly succumbed to the infection (Figure S1C). Although WT LT-HSCs did not respond to VSV int infection, infection of WT mice with a higher dose of 1×10^7 PFUs (VSV

hi) efficiently triggered transient LT-HSC activation (Figures 1C and S1D).

Next, we investigated the induction of IFN- α in blood and bone marrow during VSV infection. While VSV int infection of WT mice resulted in moderate IFN-I responses within the bone marrow, VSV hi induced substantial IFN- α levels, comparable with those observed upon poly(I:C) treatment (Figures 1D and S1E). This suggested that moderate IFN-I responses induced upon VSV int infection did not suffice to trigger LT-HSC cell cycle activation. To further study direct IFNAR triggering of LT-HSCs, we used MxCre⁺Rosa26eYFP^{ST/ST} mice that express a yellow fluorescent protein (YFP) reporter under the control of the IFN-I-stimulated Mx gene. Indeed, VSV int infection did not induce YFP expression in LT-HSCs, whereas VSV hi infection conferred enhanced YFP expression in LT-HSCs and the overall bone marrow (Figure 1E). Thus, VSV int infection of the immunocompetent host induces only moderate IFN-I responses that do not suffice to activate LT-HSCs, whereas VSV hi infection induces substantial IFN-I responses in the bone marrow that trigger HSC cell cycle entry. In contrast, in the immunocompromised host with uncontrolled virus replication, VSV int infection already leads to IFNAR-independent LT-HSC activation.

Upon Murine Cytomegalovirus Infection, LT-HSCs Are Activated in a Combination of IFNAR-Dependent and -Independent Pathways

To study an infection with high relevance for clinical bone marrow transplantation, we performed experiments with murine cytomegalovirus (MCMV), which shows more than 90% sequence homology with human CMV. We used an MCMV variant (Jordan et al., 2011) lacking the crucial natural killer (NK) cell receptor ligand m157 (Arase et al., 2002). This virus is less efficiently cleared and causes productive infection in C57BL/6 mice (Mitrović et al., 2012).

Upon infection with 5×10^5 PFUs MCMV, WT mice showed transient weight loss and survived, whereas IFNAR^{-/-} mice succumbed to the infection (Figures S2A and S2B). Of note, no peripheral blood leukopenia was detected (Figure S2C). Nevertheless, MCMV infection of WT and IFNAR^{-/-} mice resulted in massive bone marrow aplasia as well as reduced LT-HSC numbers (Figures 2A and S2D), and LT-HSCs entered the cell cycle by 4 dpi (Figure 2B). Interestingly, LT-HSC cell cycle entry was more pronounced in MCMV-infected WT mice than in IFNAR^{-/-} mice (Figures 2B and S2E), suggesting that IFNAR-dependent and -independent pathways had additive effects on LT-HSC activation. Similar to VSV infection, also MCMV-infected IFNAR^{-/-} mice showed significantly higher virus burden in peripheral organs (Figure 2C) and bone marrow than WT mice (Figure S2F).

Next, we investigated the IFN- α induction in blood and bone marrow during MCMV infection. While in MCMV-infected WT mice only slightly elevated serum IFN- α levels were detected by 1 dpi (Figure S2G), bone marrow IFN- α levels were significantly increased 1 and 4 dpi (Figure 2D). Accordingly, MCMV-infected MxCre⁺Rosa26eYFP^{ST/ST} reporter mice showed enhanced percentages of YFP expression in LT-HSCs and other bone marrow cells (Figure 2E), indicating direct IFNAR triggering of LT-HSCs upon MCMV infection. Thus, MCMV efficiently

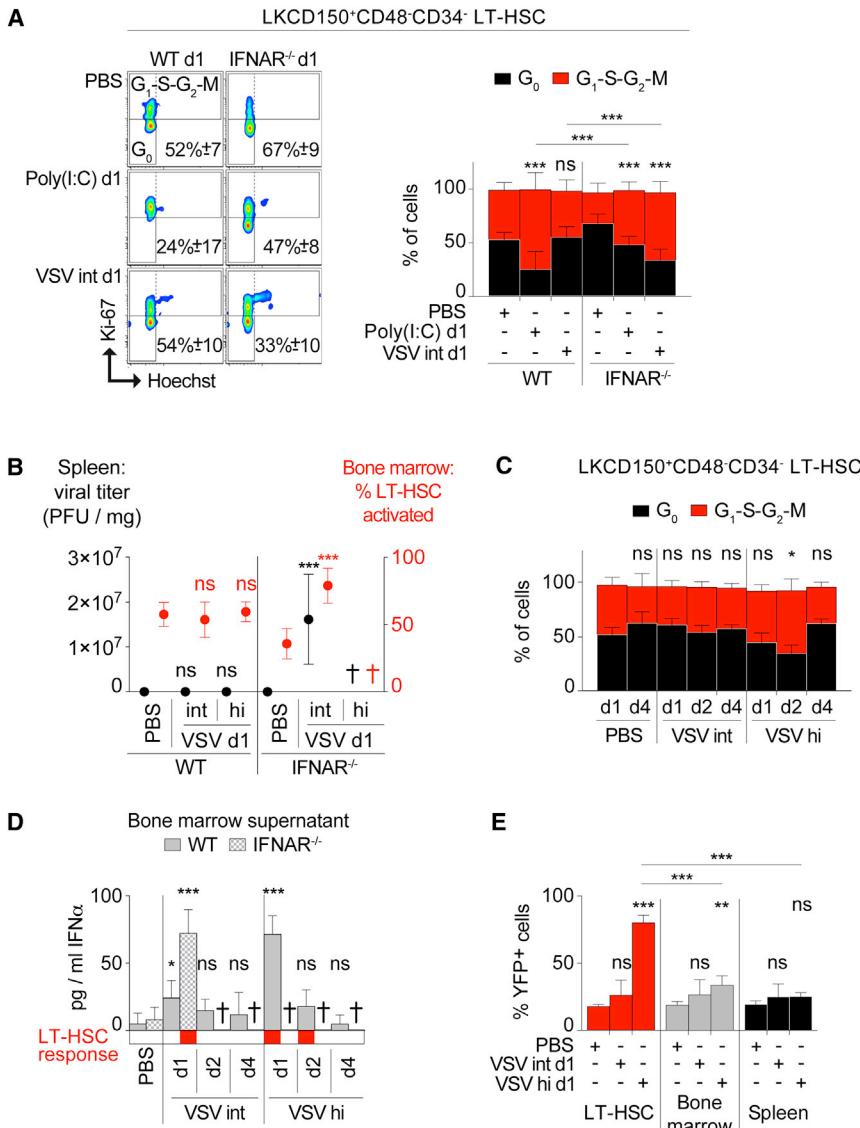


Figure 1. Challenge with High-Virus Dose or Uncontrolled Viral Replication Is Required for VSV-Induced Cell Cycle Activation of LT-HSCs

(A) Intracellular Ki-67/Hoechst staining for quiescent (G_0) and activated (G_1 -S- G_2 -M) LT-HSCs of WT and IFNAR^{-/-} mice injected i.v. with either 10 μ g/g poly(I:C) or 1 $\times 10^5$ PFUs VSV 1 dpi (n = 8–14; N = 3). Percentages in flow cytometry blots represent cells in G_0 .

(B) Correlation of peripheral virus titer (determined by plaque assay in spleen, left y axis) and activated (G_1 -S- G_2 -M) LT-HSCs (right y axis) of WT and IFNAR^{-/-} mice infected i.v. with either 1 $\times 10^5$ PFUs VSV (VSV int) or 1 $\times 10^7$ PFUs VSV (VSV hi) 1 dpi (n = 6–14; N = 2–3). Crosses indicate mice succumbing to infection.

(C) LT-HSC activation kinetics at indicated dpi of WT mice infected with either VSV int or VSV hi (n = 4–9; N = 2).

(D) IFN- α ELISA of bone marrow supernatants of mice from (A)–(C) (n = 6; N = 2). Red boxes below graph indicate coinciding LT-HSC responses (exit from quiescence). Black crosses indicate mice succumbing to infection.

(E) Percentage YFP⁺ LT-HSCs, total bone marrow, and splenocytes of MxCre⁺Rosa26eYFP^{ST/ST} mice 1 dpi with either VSV int or VSV hi (n = 5–6; N = 2). Error bars indicate mean \pm SD; significance was determined by two-sided t test or two-way ANOVA (*p \leq 0.05, **p \leq 0.0025, and ***p \leq 0.0001; ns, not significant; n, biological replicates; N, experimental repetitions).

See also Figure S1.

induces LT-HSC activation, even at an intermediate infection dose, by a combination of IFNAR-dependent and -independent pathways.

Upon Peripheral Virus Infection, LT-HSC Activation Is Conferred by Inflammatory Cytokine and Chemokine Responses in the Bone Marrow

The above data indicated that, upon VSV and MCMV infection, other signaling pathways may confer LT-HSC activation in addition to IFNAR triggering. To further characterize the corresponding inflammatory responses, we performed cytokine and chemokine arrays in serum and bone marrow of VSV- and MCMV-infected mice. VSV int infection induced a diverse inflammatory response in the serum of WT and IFNAR^{-/-} mice. However, in the bone marrow of WT mice, the response was strongly attenuated when compared with IFNAR^{-/-} mice (Figure 3A). Interestingly, only upon conditions that triggered LT-HSC activation (VSV hi

infection of WT mice or VSV int infection of IFNAR^{-/-} mice) were inflammatory responses detected within the bone marrow that included significantly increased levels of IL-10, IL-12(p40), CCL2, CCL3, and CCL4 (Figures 3A–3C). In silico analysis of published transcriptome data (Cabezas-Wallscheid et al., 2014) suggested expression of the respective cytokine and chemokine receptors on LT-HSCs, with particularly high expression of IL-10 and IL-12 receptors (Figure S3A). FACS analysis confirmed the expression of IL-10 receptor on LT-HSCs, and it showed an increased receptor expression during VSV hi infection (Figure S3B). These data support the hypothesis that the cytokines detected in the bone marrow of VSV-infected mice might directly act on LT-HSCs.

In comparison to VSV, MCMV infection of WT and IFNAR^{-/-} mice caused significantly different inflammatory responses in blood and bone marrow (Figure 3D). Nevertheless, also MCMV infection induced IL-10, IL-12(p40), CCL2, CCL3, and CCL4 within the bone marrow of WT and IFNAR^{-/-} mice at the time when LT-HSC activation was detected (Figures 3D and 3E). Thus, upon VSV as well as MCMV infection, bone marrow expression of distinct cytokines and chemokines correlates with LT-HSC activation.

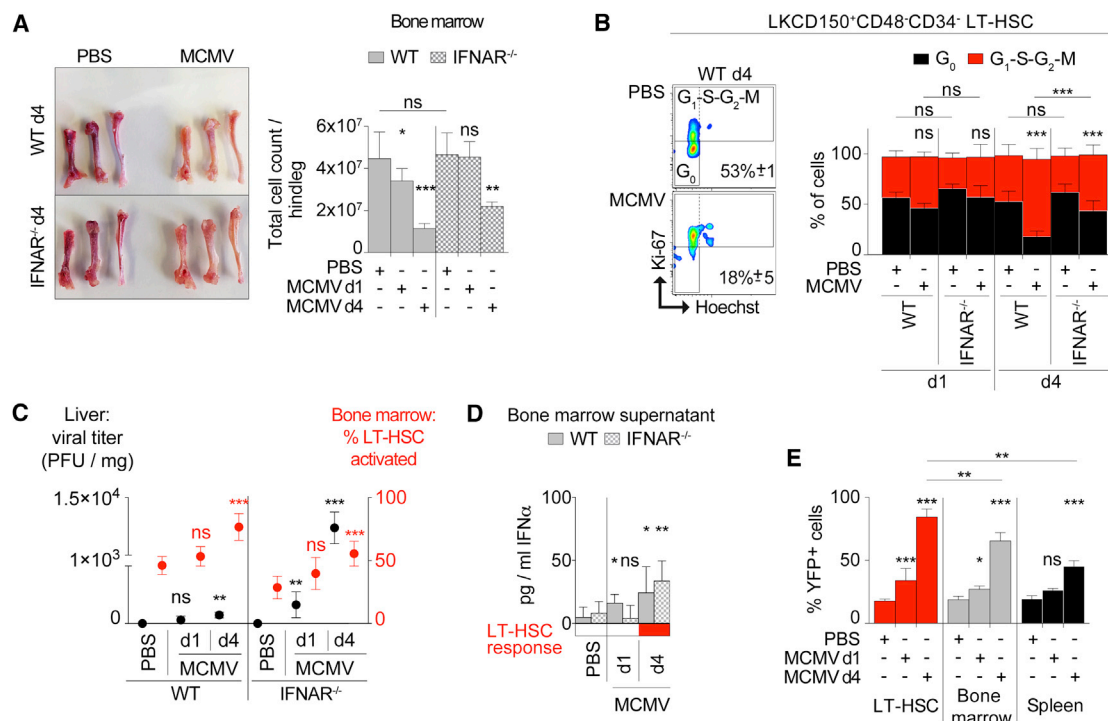


Figure 2. MCMV Infection Induces IFNAR-Independent Bone Marrow Aplasia and Readily Activates LT-HSCs

(A) Hind leg bones (hip bone, femur, tibia) of WT and IFNAR^{-/-} mice 4 dpi with 5×10^5 PFUs MCMV i.v. (left panel). Total bone marrow cell count of infected mice 1 and 4 dpi is shown (right panel; n = 4–10; N = 2).

(B) Intracellular Ki-67/Hoechst staining for quiescent (G₀) and activated (G₁-S-G₂-M) LT-HSCs 1 and 4 dpi of MCMV-infected WT and IFNAR^{-/-} mice (n = 5–9; N = 3). Percentages in flow cytometry blots represent cells in G₀.

(C) Correlation of peripheral virus titer (determined by plaque assay in liver, left y axis) and activated (G₁-S-G₂-M) LT-HSCs (right y axis) of WT and IFNAR^{-/-} mice 1 or 4 dpi with MCMV (n = 5–9; N = 2–3).

(D) IFN- α ELISA of bone marrow supernatants of mice from (B) and (C) (n = 6–13; N = 2). Red boxes below graph indicate coinciding LT-HSC responses (exit from quiescence).

(E) Percentage YFP⁺ LT-HSCs, total bone marrow, and splenocytes of MxCre⁺Rosa26eYFP^{ST/ST} mice 1 and 4 dpi with MCMV (n = 5–6; N = 2). Error bars indicate mean \pm SD; significance was determined by two-sided t test or two-way ANOVA (*p \leq 0.05, **p \leq 0.0025, and ***p \leq 0.0001; ns, not significant; n, biological replicates; N, experimental repetitions).

See also Figure S2.

Acute and Non-acute MCMV Infection of Mice Impairs Bone Marrow Reconstitution Capacity

To test whether virus-induced LT-HSC activation affects their reconstitution potential, we performed competitive bone marrow transplantation experiments with bone marrow from MCMV-infected mice. Since CMV has the potential to establish persistent infection (Pollock et al., 1997), we studied bone marrow isolated during the acute (4 dpi) and a non-acute phase of infection (21 dpi).

CD45.2⁺ WT mice were either PBS treated or MCMV infected, bone marrow was isolated at 4 or 21 dpi, mixed at a 1:1 ratio with CD45.1⁺ WT control bone marrow of untreated animals (Figure S4A), and a total of 1×10^6 cells were transplanted into lethally irradiated CD45.1⁺ WT recipients (Figure 4A). While bone marrow derived from PBS-treated controls showed similar reconstitution as bone marrow from untreated animals, bone marrow isolated 4 dpi with MCMV (4-dpi bone marrow) showed severely reduced reconstitution of all analyzed immune cell subsets up to 12 weeks post-transplantation (p.t.) (Figures 4B

and 4C). Both these experimental groups showed similar total blood cell counts (Figure S4B), indicating that the reduced engraftment of 4-dpi bone marrow was compensated by untreated CD45.1⁺ control bone marrow. To investigate whether the observed reconstitution deficits were due to impaired LT-HSC function, we performed secondary transplantations after 12 weeks. Since other bone marrow compartments do not retain their reconstitution capacity during secondary transplantation, all newly formed blood cells in these experiments were LT-HSC derived (Morrison and Weissman, 1994). In this setting, 4-dpi bone marrow still showed significantly reduced reconstitution of immune cell subsets (Figure 4D), indicating that acute MCMV infection impaired LT-HSC function.

Bone marrow prepared from MCMV-infected mice 21 dpi (21-dpi bone marrow) and transplanted at a 1:1 ratio with CD45.1⁺ WT control bone marrow from untreated mice (Figure S4C) also showed significantly reduced reconstitution up to 4 weeks p.t. compared with PBS-treated controls (Figure 4E). Also here, both experimental groups showed similar

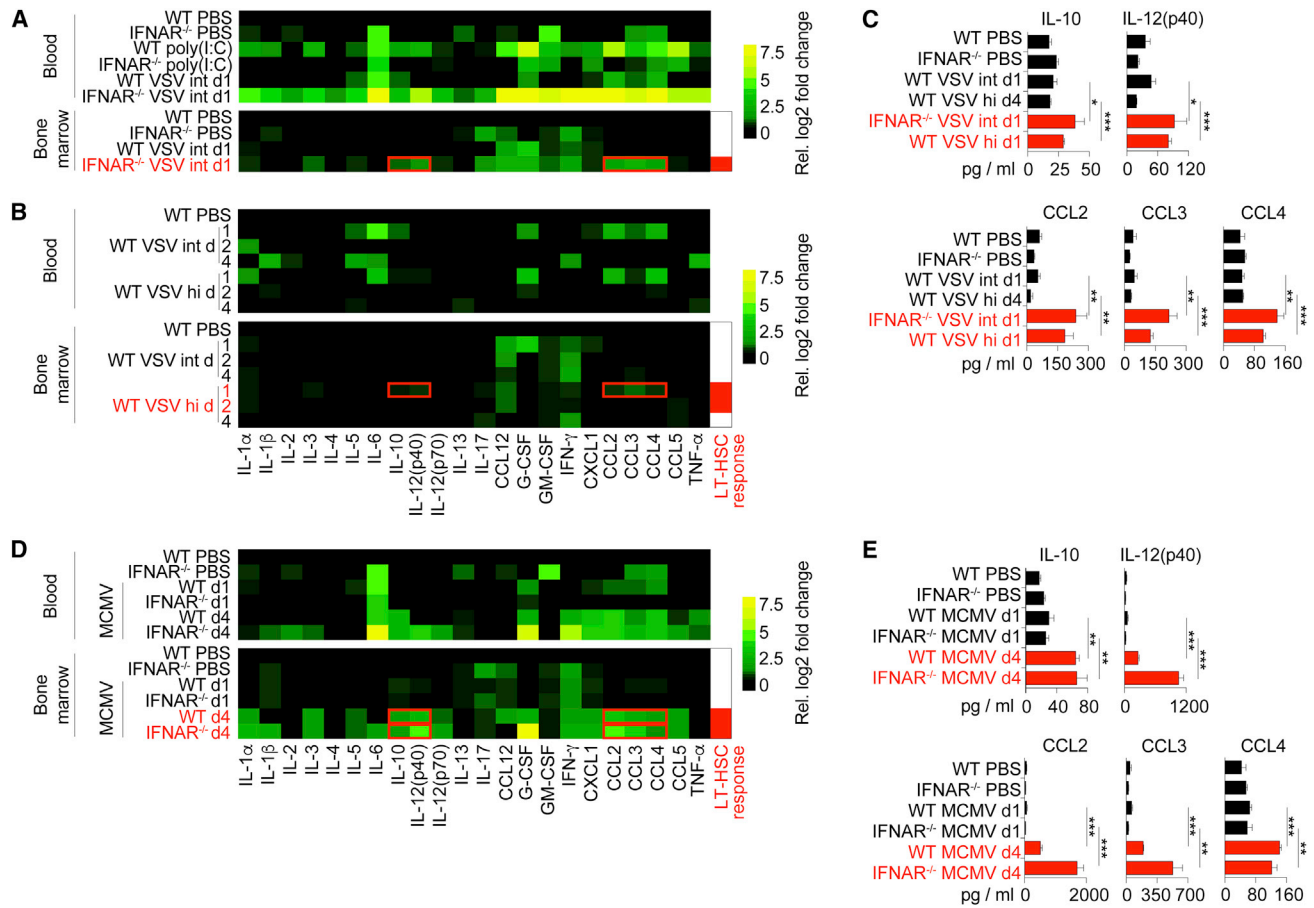


Figure 3. LT-HSC Activation upon Systemic Virus Infection Is Mediated by Inflammatory Cytokine and Chemokine Responses in the Bone Marrow

(A) Heatmaps of multiplex array for 22 cytokines and chemokines in blood sera and bone marrow supernatants of mice from Figure 1A (n = 3; N = 1). (B) Heatmaps of multiplex array for 22 cytokines and chemokines in blood sera and bone marrow supernatants of mice from Figure 1C (n = 3; N = 1). (C) Absolute values of cytokine and chemokine patterns identified in (A) and (B). (D) Heatmaps of multiplex array for 22 cytokines and chemokines in blood sera and bone marrow supernatants of mice from Figure 2B (n = 3; N = 1). (E) Absolute expression values of cytokine and chemokine patterns identified in (D). Red boxes next to heatmaps indicate coinciding LT-HSC responses (exit from quiescence). Data were normalized to WT PBS controls. Error bars indicate mean \pm SD; significance was determined by two-sided t test (* $p \leq 0.05$, ** $p \leq 0.0025$, and *** $p \leq 0.0001$; ns, not significant; n, biological replicates; N, experimental repetitions). See also Figure S3.

total blood cell counts (Figure S4D), indicating that the reduced engraftment of 21-dpi bone marrow was compensated by untreated CD45.1⁺ control bone marrow. Upon secondary transplantation, the repopulation capacity of 21-dpi bone marrow was still impaired during the initial 4 weeks (Figure 4G). Interestingly, lymphoid output was reduced for even up to 8 weeks p.t. (Figure 4F). This was associated with both a relative and absolute increase of phenotypically myeloid-biased CD150^{hi} HSCs (Beerman et al., 2010) in the bone marrow of MCMV-infected mice 21 dpi (Figure 4H). Importantly, bone marrow isolated 4 months post-MCMV infection no longer showed functional deficits (Figures S4E and S4F). In summary, acute as well as non-acute MCMV infection results in long-term, but not infinitely lasting, improper reconstitution following transplantation.

Intrinsically Impaired LT-HSCs Are the Cause of Bone Marrow Reconstitution Deficiencies following Acute and Non-acute MCMV Infection

To further confirm that impaired LT-HSCs were indeed the cause of improper reconstitution, competitive bone marrow chimeras were generated with sorted lineage⁻ c-Kit⁺ CD150⁺CD48⁻ (LKSLAM) HSCs from CD45.2⁺ donors of the respective PBS-treated or MCMV-infected (4- and 21-dpi) groups. Bone marrow mixtures of 500 CD45.2⁺ WT LKSLAM HSCs and 5×10^5 CD45.1⁺ WT control bone marrow (Figure S5A) were transplanted into lethally irradiated CD45.1⁺ WT recipients (Figure 5A). Strikingly, while by week 12 p.t. HSCs from PBS-treated mice already gave rise to nearly half of all blood cells, 4- as well as 21-dpi HSCs showed significantly reduced reconstitution (Figures 5B and 5C). Nevertheless, all experimental groups showed

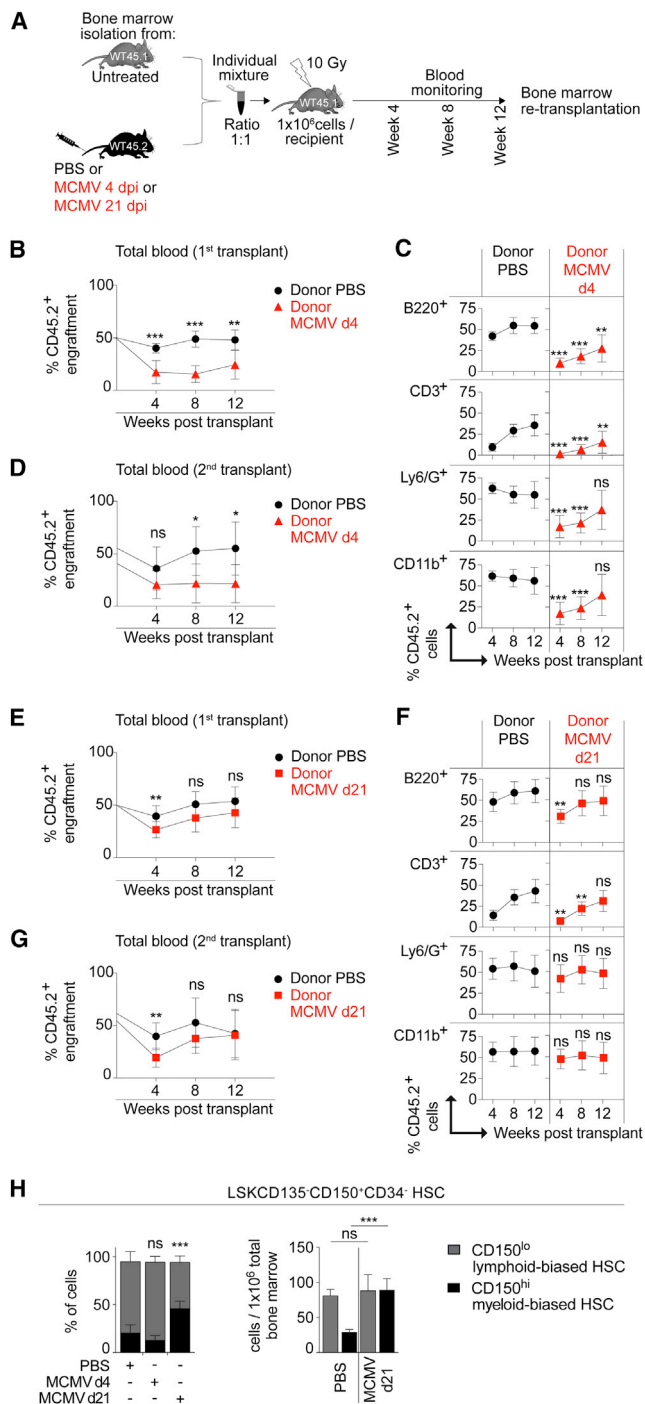


Figure 4. Bone Marrow from Mice with Acute or Non-acute MCMV Infection Shows Impaired Reconstitution Capacity

(A) Generation of competitive bone marrow chimeras and experimental layout. (B) Total blood chimerism post-transplantation from donors 4 dpi with 5×10^5 PFUs MCMV i.v. (n = 7–10; N = 2). (C) Percentage CD45.2⁺ cells in lymphoid (B220⁺ and CD3⁺) and myeloid (Ly6/G⁺ and CD11b⁺) lineages post-transplantation from (A) (n = 7–10; N = 2). (D) Second transplant of bone marrow from mice from (B), blood chimerism post-transplantation (n = 7–8; N = 2). (E) Total blood chimerism post-transplantation from donors 21 dpi with MCMV (n = 7–11; N = 2). (F) Percentage CD45.2⁺ cells in lymphoid (B220⁺ and CD3⁺) and myeloid (Ly6/G⁺ and CD11b⁺) lineages post-transplantation from (E) (n = 7–11; N = 2). (G) Second transplant of bone marrow from mice from (E), blood chimerism post-transplantation (n = 7–10; N = 2). (H) Flow cytometry analysis (at indicated time points) of LSKCD135⁺CD150⁺CD34⁺ HSCs for percentage (left panel) and absolute numbers (right panel) of CD150^{lo} lymphoid-biased and CD150^{hi} myeloid-biased HSCs of MCMV-infected WT mice (n = 5–7; N = 2). Error bars indicate mean \pm SD; significance was determined by two-sided t test (*p \leq 0.05, **p \leq 0.0025, and ***p \leq 0.0001; ns, not significant; n, biological replicates; N, experimental repetitions). See also Figure S4.

similar total blood cell counts (Figure S5B), indicating that the reduced engraftment of 4- and 21-dpi HSCs was compensated by untreated CD45.1⁺ control bone marrow. Comparable with total bone marrow transplantations, 4- as well as 21-dpi HSCs showed impaired reconstitution of immune cell lineages (Figure S5C). These data confirm that acute as well as non-acute MCMV infection of donors causes intrinsic functional LT-HSC impairment.

Non-acute MCMV Infection Is Associated with Sustained Changes in the Bone Marrow Milieu and in the LT-HSC Gene Expression Profile

To elucidate the molecular basis of LT-HSC impairment during non-acute MCMV infection, we thoroughly characterized WT mice 21 dpi. At this time point, no infectious virus particles were detected within the bone marrow (Figure S6A), while peripheral viral titers were comparable with those detected during the acute phase of the infection (4 dpi) (Figure S6B). To study whether traces of virus were nonetheless present in different bone marrow cell subsets, we performed highly sensitive qRT-PCR analyses for the most abundant MCMV transcript, *Mat* (Juranic Lisnic et al., 2013). These analyses revealed moderately elevated *Mat* expression in CD45⁺ bone marrow stroma, LKCD150⁺ committed progenitors (CPs), and LKCD150⁺CD48⁺ HSCs (LKSLAM HSCs) from MCMV-infected WT mice on 4 dpi, whereas *Mat* expression was no longer detectable by 21 dpi (Figure 6A). As expected, high *Mat* expression levels were detected in the same cell subsets as analyzed above in MCMV-infected IFNAR^{−/−} mice that showed uncontrolled virus replication (Figures 6A and S2F). Moreover, by 21 dpi, bone marrow cellularity, LT-HSC numbers (Figures 6B and S6C), and IFN- α levels in bone marrow and serum returned to steady-state levels (Figure S6D). Intriguingly, increased levels of IFN- γ , IL-17, and CCL12 remained present until 21 dpi in the bone marrow, but not in serum (Figures 6C and S6E). However, despite this local inflammatory milieu, LT-HSCs as well as CPs displayed a homeostatic cell cycle state (Figures 6D and S6F). In contrast to MCMV infection, 21 dpi with VSV hi, the bone marrow cytokine milieu and LT-HSC cell cycle state were indistinguishable from PBS-treated controls (Figures S6G and S6H). Accordingly, no reconstitution deficit was observed upon bone marrow transplantation (Figure S6I), indicating a complete remission of LT-HSC phenotype and function at later time points following VSV infection.

(E) Total blood chimerism post-transplantation from donors 21 dpi with MCMV (n = 7–11; N = 2). (F) Percentage CD45.2⁺ cells in lymphoid (B220⁺ and CD3⁺) and myeloid (Ly6/G⁺ and CD11b⁺) lineages post-transplantation from (E) (n = 7–11; N = 2). (G) Second transplant of bone marrow from mice from (E), blood chimerism post-transplantation (n = 7–10; N = 2). (H) Flow cytometry analysis (at indicated time points) of LSKCD135⁺CD150⁺CD34⁺ HSCs for percentage (left panel) and absolute numbers (right panel) of CD150^{lo} lymphoid-biased and CD150^{hi} myeloid-biased HSCs of MCMV-infected WT mice (n = 5–7; N = 2). Error bars indicate mean \pm SD; significance was determined by two-sided t test (*p \leq 0.05, **p \leq 0.0025, and ***p \leq 0.0001; ns, not significant; n, biological replicates; N, experimental repetitions). See also Figure S4.

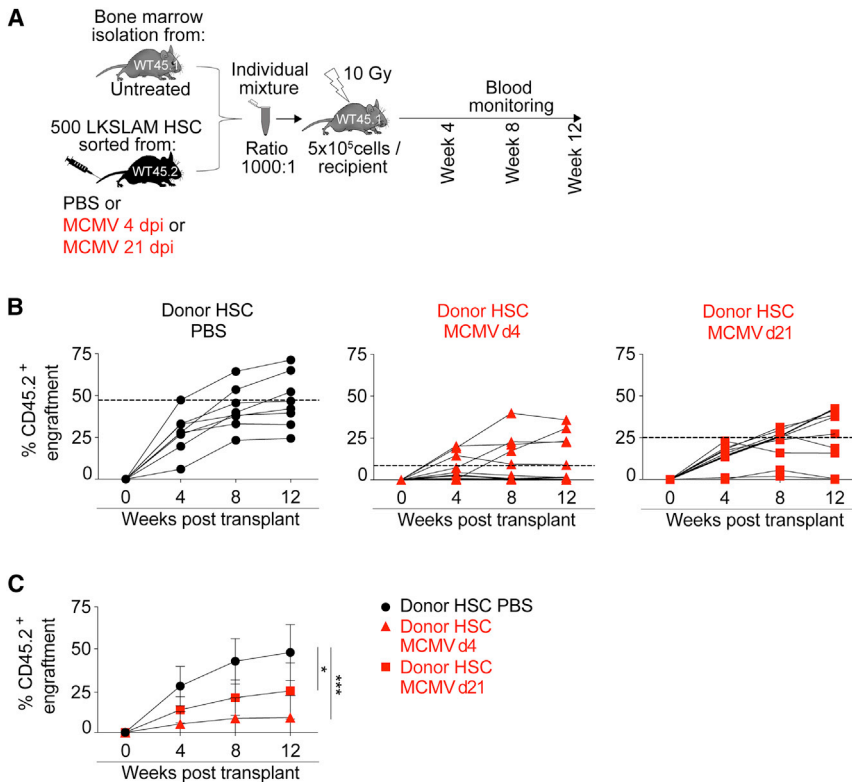


Figure 5. Intrinsic Impairment of LT-HSCs Is the Cause of Reduced Reconstitution Capacity following Acute and Non-acute MCMV Infection

(A) Generation of competitive bone marrow chimeras with sorted LKCD150⁺CD48⁺ HSCs and experimental layout.

(B) CD45.2⁺ engraftment of individual mice from (A) post-transplantation (dashed line: mean engraftment at week 12) (n = 7–14; N = 2).

(C) Quantification of data from (B). Error bars indicate mean ± SD; significance was determined by two-sided t test (*p ≤ 0.05, **p ≤ 0.0025, and ***p ≤ 0.0001; ns, not significant; n, biological replicates; N, experimental repetitions).

See also Figure S5.

found that only high-dose VSV infection activated LT-HSCs, while already moderate doses of MCMV induced transient bone marrow aplasia and LT-HSC activation. Upon all virus infections tested, cytokine patterns detected in the bone marrow differed significantly from those detected in the blood. In transplantation assays, bone marrow as well as HSCs isolated 4 days (acute phase) and 21 days (non-acute phase) after MCMV infection showed reduced capacity to

Next, we investigated whether the inflammatory milieu induced upon MCMV infection might be associated with gene expression changes in HSCs. The qRT-PCR analyses of selected IFN-I-stimulated genes (ISGs) in CPs and LKSLAM HSCs of MCMV-infected WT mice revealed that ISG (*Isg15* and *Gbp6*) expression was enhanced during the acute phase (4 dpi), but it returned back to steady-state levels by 21 dpi. In contrast, increased expression of stem cell antigen-1 (*Sca-1*) was detected in HSCs 4 dpi, but it remained elevated until 21 dpi (Figure 6E, upper panel). The expression of the quiescence enforcer *Scf* (Lacombe et al., 2010) was significantly reduced 4 dpi, but it returned to steady-state levels by 21 dpi (Figure 6E, lower panel), in line with the observed transient cell cycle induction of LT-HSCs. An increased expression of the HSC regulator *Evi1* (Kataoka et al., 2011) was detected exclusively in HSCs 21 dpi (Figure 6E, lower panel). The changes in gene expression of *Isg15* and *Evi1* were confirmed by single-cell qRT-PCR analysis of LKSLAM HSCs (Figure 6F) and verified by the analysis of housekeeping gene expression (Figure S6J). In summary, these results indicate that non-acute MCMV infection induces a sustained inflammatory milieu in the bone marrow, even when virus is absent from the hematopoietic system. This inflammatory milieu affects gene expression profiles in HSCs, and it is associated with impaired HSC function upon transplantation.

DISCUSSION

In this study, we investigated the impact of virus-induced inflammatory responses on LT-HSC phenotype and function. We

reconstitute immune cells. Notably, HSCs returned to phenotypic quiescence during non-acute MCMV infection, but they still showed altered gene expression profiles and a reduced reconstitution capacity. These findings indicate that inflammatory responses that exceed certain threshold levels in the bone marrow may induce LT-HSC activation and that a sustained inflammatory response in the bone marrow can result in long-lasting impairment of LT-HSC function (Figure 7).

An intermediate VSV dose did not induce LT-HSC activation in WT but in IFNAR^{-/-} mice. This may be due to efficient virus control in WT mice and unrestricted virus replication and highly deregulated inflammatory responses in IFNAR^{-/-} mice (Müller et al., 1994). Nevertheless, high-dose VSV challenge of WT mice efficiently activated LT-HSCs. Accordingly, MxCre⁺ Rosa26eYFP^{ST/ST} reporter mice showed direct IFNAR triggering of LT-HSCs only upon high-, but not intermediate-dose VSV infection. HSCs have been suggested to be activated either by pulls (i.e., immune cell depletion) or pushes (i.e., inflammation) (King and Goodell, 2011). Our results indicate that only VSV-induced inflammatory responses resulting from either high-dose virus infection (of WT mice) or uncontrolled viral replication (in IFNAR^{-/-} mice) exceed threshold levels within the bone marrow to efficiently push LT-HSCs into activation. Since frequent LT-HSC activation leads to apoptosis and DNA damage (Pietras et al., 2014; Walter et al., 2015), such an inflammatory threshold assures that LT-HSCs are not activated too frequently, but rather only when required, i.e., in the context of severe infections.

Interestingly, upon MCMV infection, LT-HSC activation was more pronounced in WT than in IFNAR^{-/-} mice. MCMV-induced

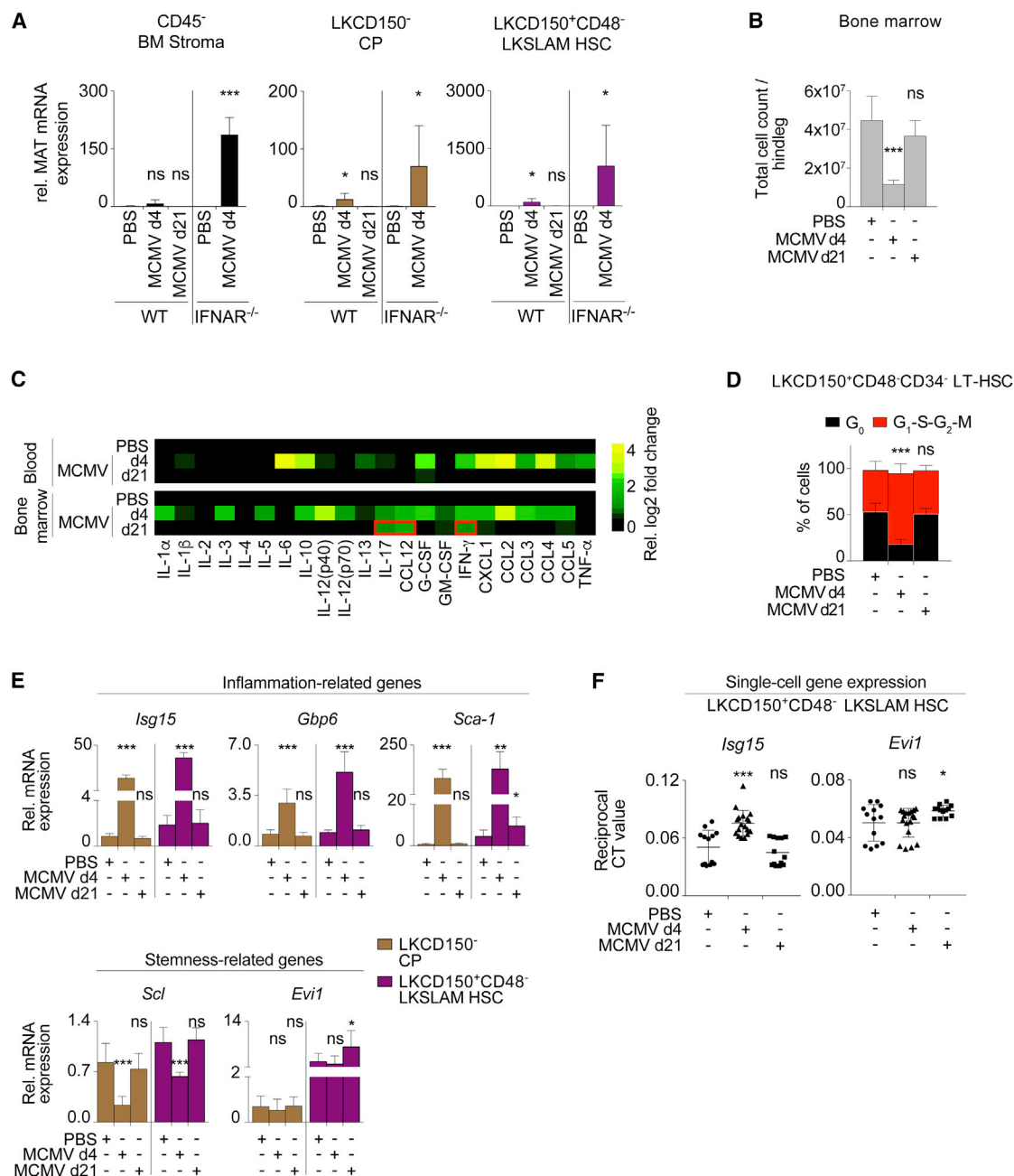


Figure 6. Impairment of LT-HSCs during Non-acute MCMV Infection Is Associated with Sustained Changes in Both the Inflammatory Milieu within the Bone Marrow as well as the LT-HSC Gene Expression Profile

(A) The qRT-PCR (at indicated time points) for the most abundant transcript (*Mat*) of MCMV in sorted CD45⁺ bone marrow stroma cells, committed progenitors (CPs), and LKSLAM HSCs (compare Figure S1A) of WT and IFNAR^{-/-} mice infected i.v. with 5×10^5 PFUs MCMV ($n = 6$; $N = 2$).

(B) Cell count of total bone marrow 4 and 21 dpi of WT mice infected i.v. with 5×10^5 PFUs MCMV ($n = 8$ –11; $N = 3$).

(C) Heatmap of multiplex array for 22 cytokines and chemokines in blood sera and bone marrow supernatants of mice from (B) ($n = 3$; $N = 1$). Data were normalized to WT PBS controls.

(D) Intracellular Ki-67/Hoechst staining for quiescent (G_0) and activated (G_1 -S- G_2 -M) LT-HSCs of MCMV-infected WT mice 4 and 21 dpi ($n = 9$ –15; $N = 3$).

(E) qRT-PCR for interferon-stimulated genes (*Isg*) (upper panels) and stemness-associated genes (lower panels) in CPs and LKSLAM HSCs of MCMV-infected WT mice 4 and 21 dpi ($n = 6$ –10; $N = 2$).

(F) Single-cell qRT-PCR for *Isg15* as well as *Evi1* in sorted LKSLAM HSCs of MCMV-infected WT mice 4 and 21 dpi ($n = 13$ –18; $N = 1$). Error bars indicate mean \pm SD; significance was determined by two-sided t test or two-way ANOVA (* $p \leq 0.05$, ** $p \leq 0.0025$, and *** $p \leq 0.0001$; ns, not significant; n, biological replicates; N, experimental repetitions).

See also Figure S6.

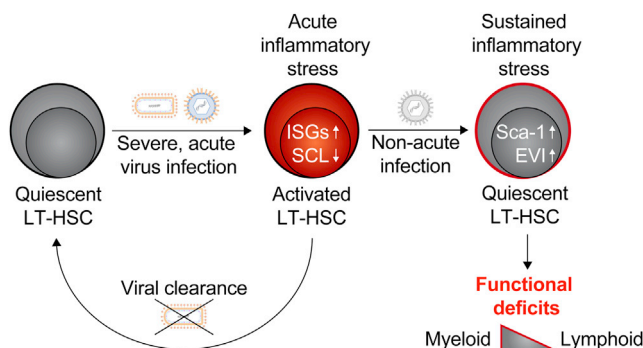


Figure 7. Working Model for the Influence of Acute and Non-acute Systemic Virus Infections on LT-HSC Phenotype and Function

If, during severe and acute virus infections, an inflammatory threshold is exceeded locally within the bone marrow, LT-HSCs show increased *Isg* levels, decreased *Scl* expression, and a subsequent activation from quiescence. If systemic infection is successfully cleared (i.e., VSV), LT-HSCs return to quiescence and regain normal function. However, non-acute systemic infections (i.e., MCMV) are capable of inducing a sustained inflammatory bone marrow milieu. As a consequence, despite their phenotypic quiescence, LT-HSCs display increased *Sca-1* as well as *Evi1* mRNA levels and functional deficits (namely, decreased lymphoid output) upon transplantation.

IFN-I responses were biologically active and directly triggered HSCs, as indicated by enhanced YFP expression in bone marrow cells of MCMV-infected *MxCre⁺Rosa26eYFP^{ST/ST}* reporter mice. Nevertheless, MCMV infection induced IFNAR-independent bone marrow aplasia, suggesting that cytokines other than IFN-I also triggered inflammatory bone marrow responses. Taken together, these experiments indicate that, while MCMV-induced LT-HSC activation can be mediated by other cytokines, IFN-I still remains a critical factor. On the one hand, particularly upon virus infections, IFN-I might push the inflammatory response above thresholds required for LT-HSC activation. On the other hand, IFNAR-independent LT-HSC activation may assure that even viruses that efficiently inhibit IFN-I (Hoffmann et al., 2015) still confer a hematopoietic push.

Of note, VSV and MCMV are two fundamentally different viruses in terms of tropism, kinetics of infection, as well as mechanisms to induce and evade cytokine responses. In the presence of IFN-I, one MCMV replication cycle takes several days (Dağ et al., 2014), explaining the delayed kinetics of MCMV-induced LT-HSC activation compared with VSV infection.

VSV infection induced cytokine and chemokine responses comprising IL-12(p40), IL-10, CCL2, CCL3, CCL4, and others, as well as an increase of IL-10 receptor expression on LT-HSCs. IL-12(p40) is produced by macrophages, neutrophils, and dendritic cells during inflammation (Hamza et al., 2010). In contrast, IL-10 is an anti-inflammatory cytokine reported to prevent immunopathology (de Vries, 1995) and to promote HSC self-renewal (Kang et al., 2007). CCL2, CCL3, and CCL4 are crucial for immune cell recruitment during infections (Castellino et al., 2006; Deshmane et al., 2009). Notably, also during MCMV infection, IL-12(p40), IL-10, CCL2, CCL3, and CCL4 were detected within the bone marrow. Thus, these mediators potentially confer LT-HSC activation either via direct triggering or indirectly through

immune cell recruitment and migration, even in the absence of functional IFNAR signaling.

MCMV is able to establish persistent infection (Pollock et al., 1997), and it has been reported to infect bone marrow stroma in BALB/c mice (Reddehase et al., 1992). The MCMV variant used in this study lacks the Ly49H ligand m157 (Arase et al., 2002), thus evading initial NK cell control to establish productive infection in C57BL/6 mice (Mitrović et al., 2012). In our experiments, in addition to the acute day 4 time point, we additionally examined WT mice in a non-acute setting 21 days after infection. During non-acute MCMV infection, virus was detected in liver, but not in bone marrow stroma, CPs, or LKSLAM HSCs (as determined by plaque assay and *Mat* expression analysis). Nevertheless, our data do not entirely exclude that very low levels of viral genomes may continue to persist in hematopoietic cells. Of note, CMV has been shown to directly interact with the genomic region of the HSC self-renewal factor *Satb1* (Lee et al., 2007) and to prevent immune cell replenishment without directly infecting HSCs (Mutter et al., 1988).

HSCs that are forced to exit from quiescence lose their long-term reconstitution capability (Orford and Scadden, 2008). Accordingly, bone marrow as well as HSCs isolated during acute MCMV infection showed severely impaired reconstitution in competitive bone marrow transplantation experiments. Importantly, also bone marrow and HSCs isolated during non-acute MCMV infection showed long-lasting, albeit transient, reconstitution deficits that mainly affected the lymphoid lineage. Interestingly, bone marrow analyzed during non-acute MCMV infection contained an increased percentage of myeloid-biased HSCs. A similar phenotype has previously been described as an aging-associated bone marrow change (Beerman et al., 2010). This suggests that aging and MCMV-induced sustained inflammation have a comparable impact on HSC differentiation bias. Interestingly, upon acute lymphocytic choriomeningitis virus (LCMV) infection, reduced myeloid differentiation was detected (Matatall et al., 2014), suggesting that, depending on the type of systemic virus infection, HSC function might be influenced differently.

In contrast to MCMV infection, VSV is efficiently controlled by IFN-I (Müller et al., 1994). Accordingly, 21 dpi with VSV hi, an inflammatory milieu was no longer detected in the bone marrow and LT-HSCs returned to quiescence. Furthermore, competitive bone marrow transplantations from VSV-infected 21-dpi donors showed normal reconstitution. This indicates that LT-HSCs may recover phenotypically and functionally once a systemic virus infection is entirely resolved.

Collectively, these findings may explain why in clinics bone marrow grafts often do not confer efficient reconstitution or even fail after an initial period of successful engraftment. Of note, similarly to infections, vaccinations can trigger acute inflammation that could potentially affect long-term hematopoietic reconstitution of bone marrow transplants. This important clinical aspect will have to be addressed experimentally in future studies.

Since during non-acute MCMV infection LT-HSCs returned to homeostatic cell cycle quiescence, we intended to analyze the mechanism causing a sustained reconstitution impairment of these cells. In accordance with their phenotypic quiescence 21 dpi with MCMV, we found LT-HSCs expressing homeostatic

levels of the quiescence enforcer *Scf*. Additionally, no bone marrow IFN- α was detectable, and the expression of hallmark ISGs (*Isg15* and *Gbp6*) in CPs and HSCs waned to steady-state levels. Nevertheless, 21 dpi a sustained inflammatory bone marrow milieu with enhanced IFN- γ , IL-17, and CCL12 levels was detected. This could be attributable to cytokine secretion by recirculating immune cells activated in peripheral lymphoid tissues. Furthermore, increased *Sca-1* mRNA levels were detected in HSCs 21 dpi. Interestingly, IFN- γ was shown to induce *Sca-1* expression in LT-HSCs (Holmes and Stanford, 2007) and, moreover, to play a key role in LT-HSC activation during chronic mycobacterial (Baldridge et al., 2010) and acute LCMV infection (Matatall et al., 2014). Of note, in both bulk as well as single-cell HSC analyses, we also found increased mRNA levels of *Evi1*, an HSC master regulator (Kataoka et al., 2011). *Evi1* was recently described as a marker of acute myeloid leukemia (AML) and chronic myeloid leukemia (CML) (Sato et al., 2014) and to be associated with poor cancer prognosis (Jo et al., 2015). Taken together, our results indicate that sustained MCMV-induced inflammatory responses within the bone marrow directly trigger LT-HSCs and, thus, affect their transcriptional profile. Since overexpression of *Evi1* in HSCs was shown to deregulate several genes that control cell division and cell self-renewal (Dickstein et al., 2010), it is tempting to speculate that chronic inflammatory stress may play a role in the genesis of cancer stem cells.

In conclusion, this study highlights that acute as well as non-acute virus infections induce inflammatory responses within the bone marrow that affect LT-HSC phenotype and function. In these responses, IFN-I is an important, but not the only, crucial factor that signals hematopoietic stress and activates quiescent LT-HSCs. Following severe virus infections, HSCs show inflammation-induced changes in gene expression that correlate with impaired hematopoietic reconstitution and are sustained for weeks during non-acute, subclinical infections. These results imply that during subclinical infections of bone marrow donors, inflammation-induced stress responses of LT-HSCs might affect their reconstitution potential, causing clinically relevant complications in transplant recipients.

EXPERIMENTAL PROCEDURES

Mice, Viruses, and Other Stimuli

IFNAR^{-/-} mice (Müller et al., 1994) were backcrossed more than 20 times on the C57BL/6 background. MxCre⁺Rosa26eYFP^{ST/ST} mice were generated by crossing MxCre⁺ (Kühn et al., 1995) and Rosa26eYFP^{ST/ST} mice (Srinivas et al., 2001). C57BL/6 mice were purchased from Harlan Winkelmann. Mice were bred under specific pathogen-free, Federation for Laboratory Animal Science Associations (FELASA) conditions at Twincore and the Helmholtz-Centre for Infection Research (HZI). Experiments were performed with female mice between 10 and 16 weeks of age and in compliance with German animal welfare regulations supervised by the Lower Saxony State Office for Consumer Production and Food Safety (LAVES). VSV-M2 (VSV) (Stojdl et al., 2003) was kindly provided by John Bell (University of Ottawa). MCMV- Δ m157 (MCMV) (Jordan et al., 2011) was provided by Stefan Jordan (Icahn School of Medicine). High-molecular-weight poly(I:C) HMW (Sigma) was administered at 10 μ g/g body weight per mouse. All stimuli were intravenously (i.v.) administered in PBS.

Cell Isolation and Flow Cytometry

Bone marrow cells were isolated by crushing hind leg bones and (if required) spinal cord in cold RPMI medium, and they were treated with red blood cell

lysis buffer (Sigma). Bone marrow was stained with anti-CD135-PE monoclonal antibody (mAb) or anti-CD48-PE mAb (both eBiosciences), or anti-IL-10R-PE mAb (or corresponding isotype control) (BioLegend), anti-CD34-AF700 mAb (eBiosciences), anti-CD150-PE-Cy5 mAb, anti-Sca-1-PE-Cy7 mAb, anti-c-Kit-APC-Cy7 mAb (all BioLegend), and anti-lineage-APC (BD Pharmingen). For proliferation staining, cells were permeabilized with Cytofix/Cytoperm and stained with anti-Ki-67-FITC mAb, corresponding isotype control (all BD Pharmingen), and Hoechst 33342 nucleic acid stain (from Life Technologies).

Blood was stained with anti-B220-PacBlue mAb, anti-CD11b-APC-Cy7 mAb (both BD Pharmingen), anti-Ly6/G-PE-Cy7 mAb (BioLegend), and anti-CD3-AF647 mAb (Caltag) and treated with red blood cell lysing solution (BD Pharmingen).

Unspecific Fc-receptor binding was blocked by anti-CD16/CD32-unconjugated mAb (BD Pharmingen) prior to surface staining.

Cell counts were determined using AccuCheck counting beads (Life Technologies).

Cells were measured by flow cytometry (FACS) (LSR II Sorb; Becton Dickinson), and data were analyzed with the FlowJo software.

Cell Sorting

After bone marrow isolation, cells were lineage depleted by AutoMACS-based magnetic separation using a mouse lineage depletion kit (Miltenyi Biotec). Cells were stained with anti-CD48-PE mAb (eBioscience), anti-c-Kit-APC-Cy7 mAb, anti-CD150-PE-Cy5 mAb, and anti-lineage-PacBlue (BioLegend). Cells were sorted using a MoFlo XDP (Beckman Coulter) or Aria II (Beckton Dickinson) cell sorter.

Bone Marrow Chimeras

For 1:1 competitive bone marrow chimeras, 5×10^5 bone marrow cells from PBS- or virus-treated CD45.2⁺ WT donors were mixed with 5×10^5 bone marrow cells from CD45.1⁺ naive congenic WT donors. The 1×10^6 mixture cells were i.v. transplanted into lethally irradiated (10 Gy X-ray, 3-hr split dose) congenic CD45.1⁺ WT recipients.

For 1:1,000 competitive HSC chimeras, 500 sorted LKSLAM HSCs from PBS- or virus-treated CD45.2⁺ WT donors were mixed with 5×10^5 bone marrow cells from CD45.1⁺ naive congenic WT donors. The 5×10^5 mixture cells were i.v. transplanted into lethally irradiated congenic CD45.1⁺ WT recipients. Chimerism was determined by flow cytometry staining with anti-CD45.1-FITC mAb (BD Pharmingen) and anti-CD45.2-PacBlue mAb (BioLegend).

Bone Marrow Supernatants

Hindleg bones were crushed in 500 μ L cold RPMI medium, and suspensions were high-speed centrifuged in blood serum tubes to separate cellular components.

Cytokine and Chemokine Analyses

Serum and bone marrow supernatants were tested for IFN- α using the VeriKine kit (PBL Assay Science) and for IFN- γ using the Ready-SET-Go! kit (eBioscience), following the manufacturers' instructions. Multiplex cytokine array was performed using the Bio-Plex Pro Mouse Cytokine 23-Plex Assay (Bio-Rad), following the manufacturer's instructions. Heatmaps were generated from average values of each parameter using The R Project for Statistical Computing software.

Plaque Assays

Organ homogenates were plated in serial log10 dilutions on Vero cells for 1 day (VSV) or on mouse embryonic fibroblasts for 6–7 days (MCMV), with a 1% methyl-cellulose overlay. Plaques were counted following staining with crystal violet (Merck).

Real-Time qPCR

For bulk analyses, 5,000–15,000 CPs or HSCs were sorted into lysis buffer, and RNA was extracted using the Arcturus PicoPure kit (Applied Biosystems), according to the manufacturer's instructions. Subsequently, RNA was reverse-transcribed to cDNA using the PrimeScript Kit (Takara Clonetechn). RT-PCRs were carried out in technical triplicates using Power SYBR Green

(Applied Biosystems), and they were run on a ViiATM 7 Real-Time PCR system (Applied Biosystems). Expression values were calculated using the $\Delta\Delta CT$ method with *Sdha*, *Oaz1*, and *Actb* as endogenous control genes. Single-cell qRT-PCR experiments and analyses were performed as previously described (Haas et al., 2015). Primers for the respective experiments are listed in Table S1.

Statistical Analysis

Statistical significance was determined by two-sided t test or, for multiple data comparisons, by two-way ANOVA with Bonferroni correction. The p values are as follows: *p \leq 0.05, **p \leq 0.0025, and ***p \leq 0.0001. The number of biological replicates (n) and experimental repetitions (N) is indicated in each figure legend. All statistical analyses were performed using the GraphPad Prism 7 software.

SUPPLEMENTAL INFORMATION

Supplemental Information includes six figures and one table and can be found with this article online at <http://dx.doi.org/10.1016/j.celrep.2017.05.063>.

AUTHOR CONTRIBUTIONS

C.H., S.F.H., T.F., M.A.G.E., and U.K. conceived experiments. C.H., S.F.H., M.D., T.F., P.-K.T., K.B., C.C., E.P., and S.L. performed experiments. C.H., T.F., S.F.H., and U.K. wrote the manuscript. U.K., M.A.G.E., and A.T. secured funding. S. Jordan provided reagents. C.S.F., I.B., K.K., M.M., S. Jonjic, and S. Jordan provided expertise and feedback.

ACKNOWLEDGMENTS

We thank Matthias Ballmaier, Christina Struckmann, Marcus Eich, and Klaus Hexel for cell sorting, as well as Nadine Thiel, Vanda Juranic Lisnic, and Franziska Pilz for assistance with MCMV assays. This study was supported by funding from the Helmholtz Virtual Institute (VH-VI-424 Viral Strategies of Immune Evasion) to M.M., S. Jordan, and U.K., by funding from the Niedersachsen-Research Network on Neuroinfectiology (N-RENNT) of the Ministry of Science and Culture of Lower Saxony, Germany, to U.K., and by funding from the Hannover Biomedical Research School (HBRS) and the Centre for Infection Biology (ZIB) to C.H. S.L. was supported by a travel grant of the REBIRTH Cluster of Excellence, Hannover.

Received: March 3, 2016

Revised: April 25, 2017

Accepted: May 18, 2017

Published: June 13, 2017

REFERENCES

- Arase, H., Mocarski, E.S., Campbell, A.E., Hill, A.B., and Lanier, L.L. (2002). Direct recognition of cytomegalovirus by activating and inhibitory NK cell receptors. *Science* 296, 1323–1326.
- Baldrige, M.T., King, K.Y., Boles, N.C., Weksberg, D.C., and Goodell, M.A. (2010). Quiescent hematopoietic stem cells are activated by IFN- γ in response to chronic infection. *Nature* 465, 793–797.
- Beerman, I., Bhattacharya, D., Zandi, S., Sigvardsson, M., Weissman, I.L., Bryder, D., and Rossi, D.J. (2010). Functionally distinct hematopoietic stem cells modulate hematopoietic lineage potential during aging by a mechanism of clonal expansion. *Proc. Natl. Acad. Sci. USA* 107, 5465–5470.
- Boeckh, M., and Nichols, W.G. (2004). The impact of cytomegalovirus serostatus of donor and recipient before hematopoietic stem cell transplantation in the era of antiviral prophylaxis and preemptive therapy. *Blood* 103, 2003–2008.
- Cabezas-Wallscheid, N., Klimmeck, D., Hansson, J., Lipka, D.B., Reyes, A., Wang, Q., Weichenhan, D., Lier, A., von Paleske, L., Renders, S., et al. (2014). Identification of regulatory networks in HSCs and their immediate progeny via integrated proteome, transcriptome, and DNA methylome analysis. *Cell Stem Cell* 15, 507–522.
- Castellino, F., Huang, A.Y., Altan-Bonnet, G., Stoll, S., Scheinecker, C., and Germain, R.N. (2006). Chemokines enhance immunity by guiding naive CD8+ T cells to sites of CD4+ T cell-dendritic cell interaction. *Nature* 440, 890–895.
- Crouse, J., Kalinke, U., and Oxenius, A. (2015). Regulation of antiviral T cell responses by type I interferons. *Nat. Rev. Immunol.* 15, 231–242.
- Dağ, F., Dölken, L., Holzki, J., Drabig, A., Weingärtner, A., Schwerk, J., Lienenklaus, S., Conte, I., Geffers, R., Davenport, C., et al. (2014). Reversible silencing of cytomegalovirus genomes by type I interferon governs virus latency. *PLoS Pathog.* 10, e1003962.
- de Vries, J.E. (1995). Immunosuppressive and anti-inflammatory properties of interleukin 10. *Ann. Med.* 27, 537–541.
- Deshmane, S.L., Kremlev, S., Amini, S., and Sawaya, B.E. (2009). Monocyte chemoattractant protein-1 (MCP-1): an overview. *J. Interferon Cytokine Res.* 29, 313–326.
- Dickstein, J., Senyuk, V., Premanand, K., Laricchia-Robbio, L., Xu, P., Cattaneo, F., Fazzina, R., and Nucifora, G. (2010). Methylation and silencing of miRNA-124 by EVI1 and self-renewal exhaustion of hematopoietic stem cells in murine myelodysplastic syndrome. *Proc. Natl. Acad. Sci. USA* 107, 9783–9788.
- Essers, M.A., Offner, S., Blanco-Bose, W.E., Waibler, Z., Kalinke, U., Duchosal, M.A., and Trumpp, A. (2009). IFN α activates dormant hematopoietic stem cells in vivo. *Nature* 458, 904–908.
- Fries, B.C., Riddell, S.R., Kim, H.W., Corey, L., Dahlgren, C., Woolfrey, A., and Boeckh, M. (2005). Cytomegalovirus disease before hematopoietic cell transplantation as a risk for complications after transplantation. *Biol. Blood Marrow Transplant.* 11, 136–148.
- Haas, S., Hansson, J., Klimmeck, D., Loeffler, D., Velten, L., Uckelmann, H., Wurzer, S., Prendergast, A.M., Schnell, A., Hexel, K., et al. (2015). Inflammation-Induced Emergency Megakaryopoiesis Driven by Hematopoietic Stem Cell-like Megakaryocyte Progenitors. *Cell Stem Cell* 17, 422–434.
- Hamza, T., Barnett, J.B., and Li, B. (2010). Interleukin 12 a key immunoregulatory cytokine in infection applications. *Int. J. Mol. Sci.* 11, 789–806.
- Hoffmann, H.H., Schneider, W.M., and Rice, C.M. (2015). Interferons and viruses: an evolutionary arms race of molecular interactions. *Trends Immunol.* 36, 124–138.
- Holmes, C., and Stanford, W.L. (2007). Concise review: stem cell antigen-1: expression, function, and enigma. *Stem Cells* 25, 1339–1347.
- Jo, A., Mitani, S., Shiba, N., Hayashi, Y., Hara, Y., Takahashi, H., Tsukimoto, I., Tawa, A., Horibe, K., Tomizawa, D., et al. (2015). High expression of EVI1 and MEL1 is a compelling poor prognostic marker of pediatric AML. *Leukemia* 29, 1076–1083.
- Jordan, S., Krause, J., Prager, A., Mitrovic, M., Jonjic, S., Koszinowski, U.H., and Adler, B. (2011). Virus progeny of murine cytomegalovirus bacterial artificial chromosome pSM3fr show reduced growth in salivary Glands due to a fixed mutation of MCK-2. *J. Virol.* 85, 10346–10353.
- Juranic Lisnic, V., Babic Cac, M., Lisnic, B., Trsan, T., Mefferd, A., Das Mukhopadhyay, C., Cook, C.H., Jonjic, S., and Trgovcich, J. (2013). Dual analysis of the murine cytomegalovirus and host cell transcriptomes reveal new aspects of the virus-host cell interface. *PLoS Pathog.* 9, e1003611.
- Kang, Y.J., Yang, S.J., Park, G., Cho, B., Min, C.K., Kim, T.Y., Lee, J.S., and Oh, I.H. (2007). A novel function of interleukin-10 promoting self-renewal of hematopoietic stem cells. *Stem Cells* 25, 1814–1822.
- Kataoka, K., Sato, T., Yoshimi, A., Goyama, S., Tsuruta, T., Kobayashi, H., Shimabe, M., Arai, S., Nakagawa, M., Imai, Y., et al. (2011). Evf1 is essential for hematopoietic stem cell self-renewal, and its expression marks hematopoietic cells with long-term multilineage repopulating activity. *J. Exp. Med.* 208, 2403–2416.
- Kiel, M.J., Yilmaz, O.H., Iwashita, T., Yilmaz, O.H., Terhorst, C., and Morrison, S.J. (2005). SLAM family receptors distinguish hematopoietic stem and progenitor cells and reveal endothelial niches for stem cells. *Cell* 121, 1109–1121.

- King, K.Y., and Goodell, M.A. (2011). Inflammatory modulation of HSCs: viewing the HSC as a foundation for the immune response. *Nat. Rev. Immunol.* **11**, 685–692.
- Kühn, R., Schwenk, F., Aguet, M., and Rajewsky, K. (1995). Inducible gene targeting in mice. *Science* **269**, 1427–1429.
- Lacombe, J., Herblot, S., Rojas-Sutterlin, S., Haman, A., Barakat, S., Iscove, N.N., Sauvageau, G., and Hoang, T. (2010). Scl regulates the quiescence and the long-term competence of hematopoietic stem cells. *Blood* **115**, 792–803.
- Lee, J., Klase, Z., Gao, X., Caldwell, J.S., Stinski, M.F., Kashanchi, F., and Chao, S.H. (2007). Cellular homeoproteins, SATB1 and CDP, bind to the unique region between the human cytomegalovirus UL127 and major immediate-early genes. *Virology* **366**, 117–125.
- Matatall, K.A., Shen, C.C., Challen, G.A., and King, K.Y. (2014). Type II interferon promotes differentiation of myeloid-biased hematopoietic stem cells. *Stem Cells* **32**, 3023–3030.
- Mitrović, M., Arapović, J., Jordan, S., Fodil-Cornu, N., Ebert, S., Vidal, S.M., Krmpotić, A., Reddehase, M.J., and Jonjić, S. (2012). The NK cell response to mouse cytomegalovirus infection affects the level and kinetics of the early CD8(+) T-cell response. *J. Virol.* **86**, 2165–2175.
- Morrison, S.J., and Scadden, D.T. (2014). The bone marrow niche for haematopoietic stem cells. *Nature* **505**, 327–334.
- Morrison, S.J., and Weissman, I.L. (1994). The long-term repopulating subset of hematopoietic stem cells is deterministic and isolatable by phenotype. *Immunity* **1**, 661–673.
- Müller, U., Steinhoff, U., Reis, L.F., Hemmi, S., Pavlovic, J., Zinkernagel, R.M., and Aguet, M. (1994). Functional role of type I and type II interferons in antiviral defense. *Science* **264**, 1918–1921.
- Mutter, W., Reddehase, M.J., Busch, F.W., Bühring, H.J., and Koszinowski, U.H. (1988). Failure in generating hemopoietic stem cells is the primary cause of death from cytomegalovirus disease in the immunocompromised host. *J. Exp. Med.* **167**, 1645–1658.
- Nagai, Y., Garrett, K.P., Ohta, S., Bahrun, U., Kouro, T., Akira, S., Takatsu, K., and Kinrade, P.W. (2006). Toll-like receptors on hematopoietic progenitor cells stimulate innate immune system replenishment. *Immunity* **24**, 801–812.
- Orford, K.W., and Scadden, D.T. (2008). Deconstructing stem cell self-renewal: genetic insights into cell-cycle regulation. *Nat. Rev. Genet.* **9**, 115–128.
- Osawa, M., Hanada, K., Hamada, H., and Nakauchi, H. (1996). Long-term lymphohematopoietic reconstitution by a single CD34-low/negative hematopoietic stem cell. *Science* **273**, 242–245.
- Pietras, E.M., Lakshminarasimhan, R., Techner, J.M., Fong, S., Flach, J., Binnewies, M., and Passegué, E. (2014). Re-entry into quiescence protects hematopoietic stem cells from the killing effect of chronic exposure to type I interferons. *J. Exp. Med.* **211**, 245–262.
- Pollock, J.L., Presti, R.M., Paetzold, S., and Virgin, H.W., 4th. (1997). Latent murine cytomegalovirus infection in macrophages. *Virology* **227**, 168–179.
- Reddehase, M.J., Dreher-Stumpp, L., Angele, P., Baltesen, M., and Susa, M. (1992). Hematopoietic stem cell deficiency resulting from cytomegalovirus infection of bone marrow stroma. *Ann. Hematol.* **64** (Suppl.), A125–A127.
- Sato, T., Goyama, S., Kataoka, K., Nasu, R., Tsuruta-Kishino, T., Kagoya, Y., Nukina, A., Kumagai, K., Kubota, N., Nakagawa, M., et al. (2014). Evi1 defines leukemia-initiating capacity and tyrosine kinase inhibitor resistance in chronic myeloid leukemia. *Oncogene* **33**, 5028–5038.
- Srinivas, S., Watanabe, T., Lin, C.S., William, C.M., Tanabe, Y., Jessell, T.M., and Costantini, F. (2001). Cre reporter strains produced by targeted insertion of EYFP and ECFP into the ROSA26 locus. *BMC Dev. Biol.* **1**, 4.
- Stojdl, D.F., Lichty, B.D., tenOever, B.R., Paterson, J.M., Power, A.T., Knowles, S., Marius, R., Reynard, J., Poliquin, L., Atkins, H., et al. (2003). VSV strains with defects in their ability to shutdown innate immunity are potent systemic anti-cancer agents. *Cancer Cell* **4**, 263–275.
- Takizawa, H., Regoes, R.R., Boddupalli, C.S., Bonhoeffer, S., and Manz, M.G. (2011). Dynamic variation in cycling of hematopoietic stem cells in steady state and inflammation. *J. Exp. Med.* **208**, 273–284.
- Waibler, Z., Detje, C.N., Bell, J.C., and Kalinke, U. (2007). Matrix protein mediated shutdown of host cell metabolism limits vesicular stomatitis virus-induced interferon-alpha responses to plasmacytoid dendritic cells. *Immunobiology* **212**, 887–894.
- Walter, D., Lier, A., Geiselhart, A., Thalheimer, F.B., Huntscha, S., Sobotta, M.C., Moehle, B., Brocks, D., Bayindir, I., Kaschutnig, P., et al. (2015). Exit from dormancy provokes DNA-damage-induced attrition in haematopoietic stem cells. *Nature* **520**, 549–552.
- Wilson, A., Oser, G.M., Jaworski, M., Blanco-Bose, W.E., Laurenti, E., Adolphe, C., Essers, M.A., Macdonald, H.R., and Trumpp, A. (2007). Dormant and self-renewing hematopoietic stem cells and their niches. *Ann. N Y Acad. Sci.* **1106**, 64–75.
- Wilson, A., Laurenti, E., Oser, G., van der Wath, R.C., Blanco-Bose, W., Jaworski, M., Offner, S., Dunant, C.F., Eshkind, L., Bockamp, E., et al. (2008). Hematopoietic stem cells reversibly switch from dormancy to self-renewal during homeostasis and repair. *Cell* **135**, 1118–1129.

Supplemental Information

**Systemic Virus Infections Differentially Modulate
Cell Cycle State and Functionality of Long-Term
Hematopoietic Stem Cells In Vivo**

Christoph Hirche, Theresa Frenz, Simon F. Haas, Marius Döring, Katharina Borst, Pia-K. Tegtmeyer, Ilija Brizic, Stefan Jordan, Kirsten Keyser, Chintan Chhatbar, Eline Pronk, Shuiping Lin, Martin Messerle, Stipan Jonjic, Christine S. Falk, Andreas Trumpp, Marieke A.G. Essers, and Ulrich Kalinke

Supplementary Figures, Tables & Legends

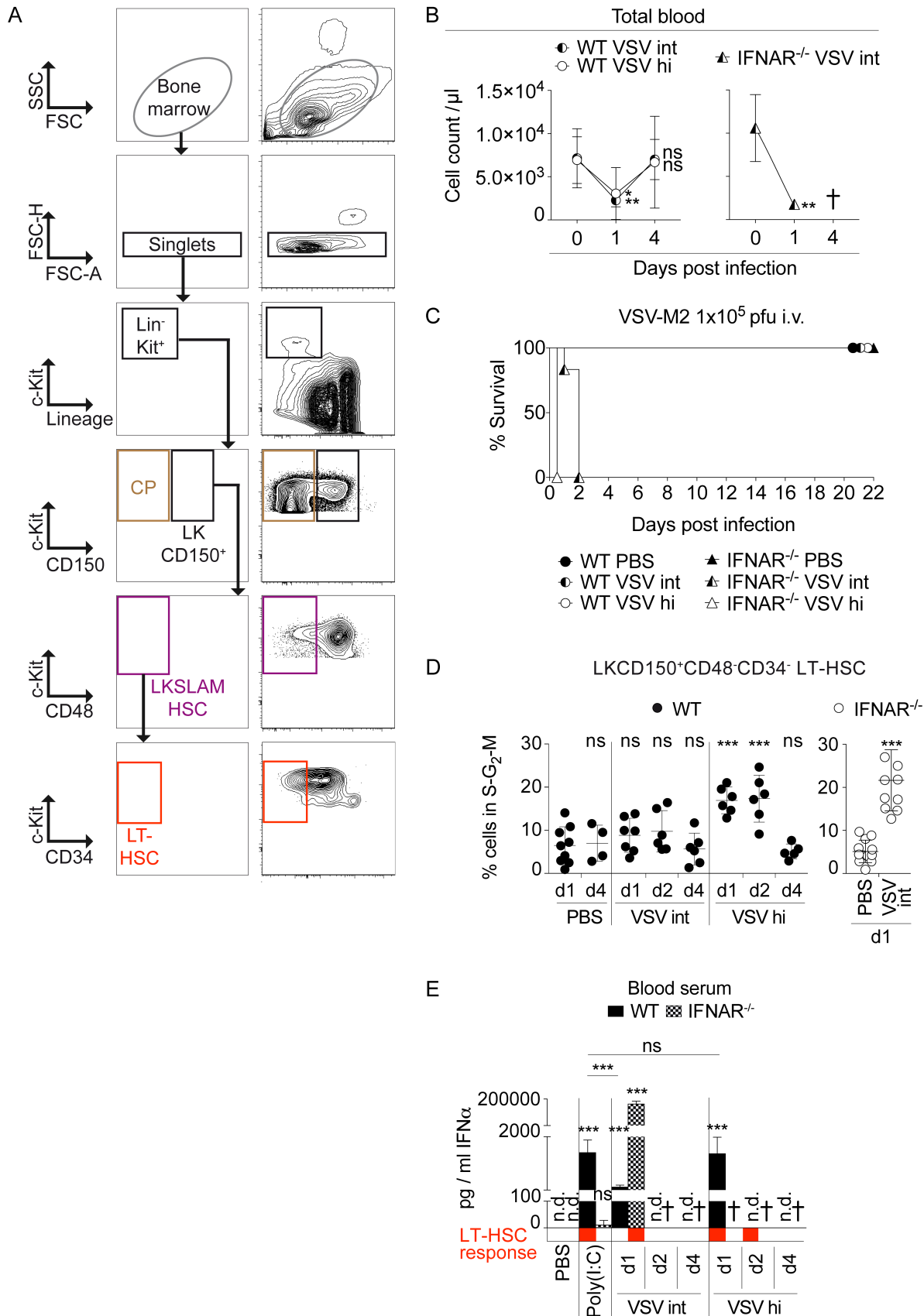


Figure S1 (related to Figure 1):

(A) Flow-cytometry gating strategy for the phenotypic characterization of Lin⁻Kit⁺CD150⁻ committed progenitors (CPs), Lin⁻Kit⁺CD150⁺CD48⁻ hematopoietic stem cells (LKSLAM HSCs) and Lin⁻Kit⁺CD150⁺CD48⁻CD34⁻ long-term hematopoietic stem cells (LT-HSCs) in the murine bone marrow. Stem cell antigen 1 (Sca-1) was excluded from gating to avoid inflammation-induced contamination of investigated bone marrow subsets (see also: Haas et al., 2015). (B) Total blood cell count kinetics of WT and IFNAR^{-/-} mice infected i.v. with either 1x10⁵ PFU VSV (VSV int) or 1x10⁷ PFU VSV (VSV hi) 1 and 4 dpi (n = 5 - 6 ; N = 2). Black cross indicates mice succumbing to infection. (C) Survival kinetics of WT and IFNAR^{-/-} mice infected i.v. with either VSV int or VSV hi (n = 5 - 6 ; N = 2). (D) Kinetics of LT-HSCs in S-G₂-M following i.v. infection of mice with either VSV int (WT and IFNAR^{-/-} mice) or VSV hi (WT mice)(n = 4-9 ; N = 2). (E) IFN-α ELISA of blood sera of mice from (D) (n = 6 ; N = 2). Red boxes below graph indicate coinciding LT-HSC responses (exit from quiescence). Black crosses indicate mice succumbing to infection. Error bars indicate mean±SD, significance determined by two-sided t-test (*, p≤0.05; **, p≤0.0025; ***, p≤0.0001; ns = not significant; n = biological replicates; N = experimental repetitions).

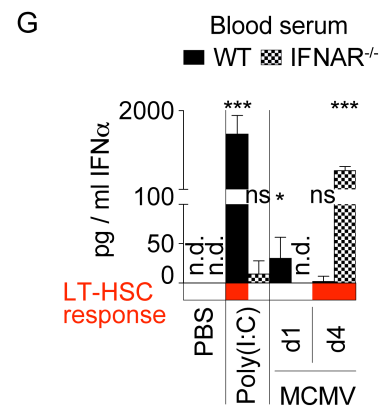
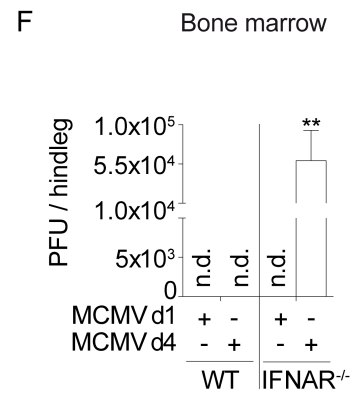
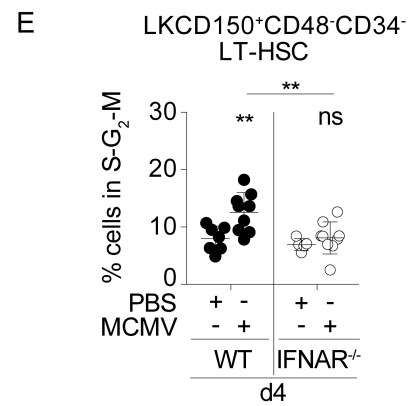
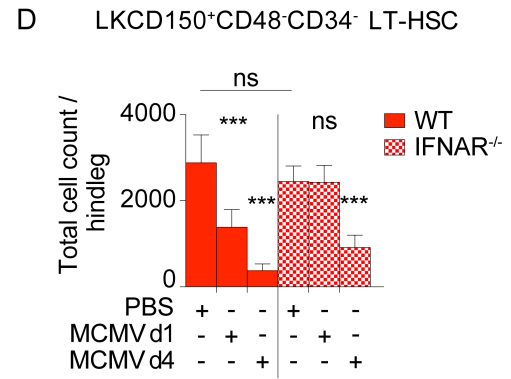
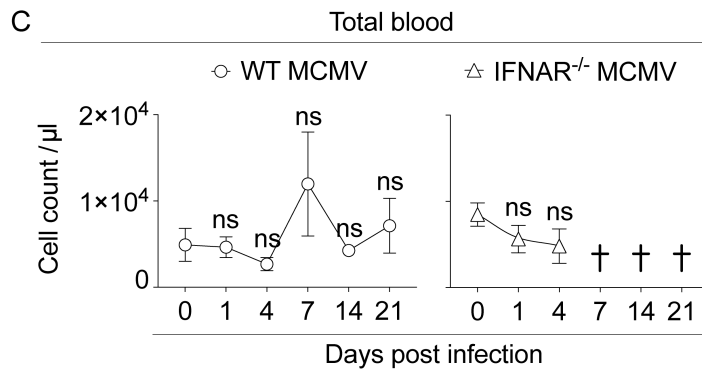
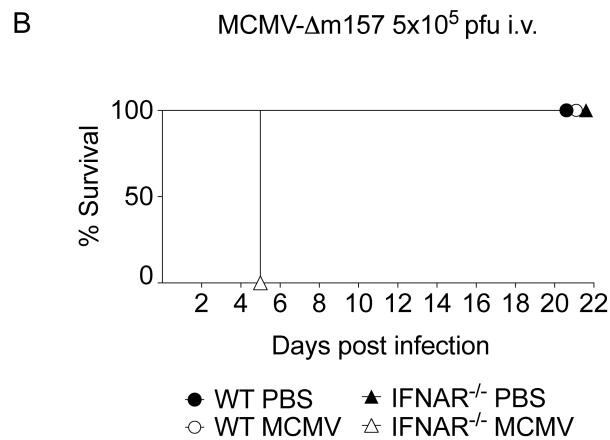
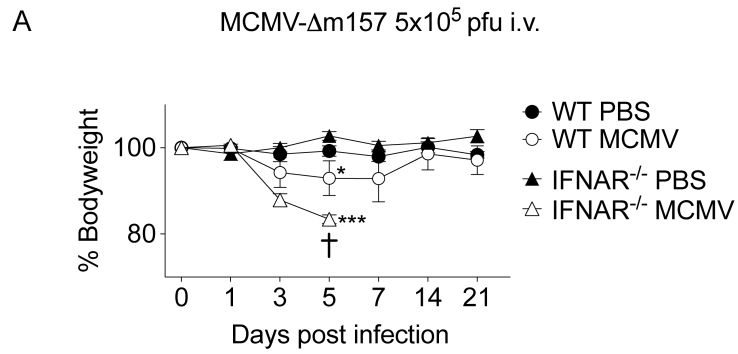


Figure S2 (related to Figure 2):

(A) Weight loss kinetics of WT and IFNAR^{-/-} mice infected i.v. with 5x10⁵ PFU MCMV (n = 3 - 6 ; N = 2). Black cross indicates mice succumbing to infection. **(B)** Survival kinetics of MCMV-infected WT and IFNAR^{-/-} mice (n = 3 - 6 ; N = 2). **(C)** Total blood cell count kinetics of MCMV-infected WT and IFNAR^{-/-} mice (n = 3 - 6 ; N = 2). Black cross indicates mice succumbing to infection. **(D)** Cell count of LT-HSCs of MCMV-infected WT and IFNAR^{-/-} mice 1 and 4 dpi (n = 4-10 ; N = 2). **(E)** Percentages of LT-HSCs in S-G₂-M following MCMV infection of WT and IFNAR^{-/-} mice 4 dpi (n = 5-9 ; N = 2-3). **(F)** Viral titers determined by plaque assay 1 and 4 dpi in bone marrow of MCMV-infected WT and IFNAR^{-/-} mice (n = 6 ; N = 2). **(G)** IFN-α ELISA of blood sera of MCMV-infected WT and IFNAR^{-/-} mice 1 and 4 dpi (n = 6-13 ; N = 2). Red boxes below graph indicate coinciding LT-HSC responses (exit from quiescence). Error bars indicate mean±SD, significance determined by two-sided t-test (*, p≤0.05; **, p≤0.0025; ***, p≤0.0001; ns = not significant; n = biological replicates; N = experimental repetitions).

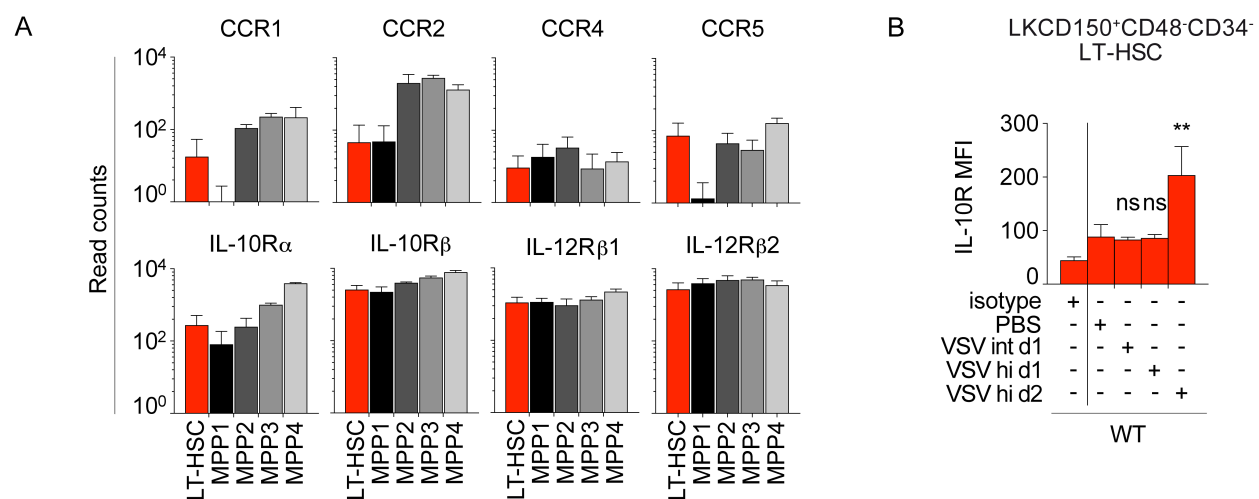


Figure S3 (related to Figure 3):

(A) *In silico* analysis of published transcriptome data of LT-HSCs as well as downstream multipotent progenitor populations (MPP 1-4) (Cabezas-Wallscheid et al., 2014) for the expression of CCL2, CCL3, CCL4 (upper panels) as well as IL-10 and IL-12 (lower panels) cytokine and chemokine receptors. **(B)** IL-10 receptor expression in WT mice following infection with either 1×10^5 PFU VSV (VSV int) or 1×10^7 PFU VSV (VSV hi) at indicated time points ($n = 4-6$; $N = 2$). Error bars indicate mean \pm SD, significance determined by two-sided t-test (*, $p \leq 0.05$; **, $p \leq 0.0025$; ***, $p \leq 0.0001$; ns = not significant; n = biological replicates; N = experimental repetitions).

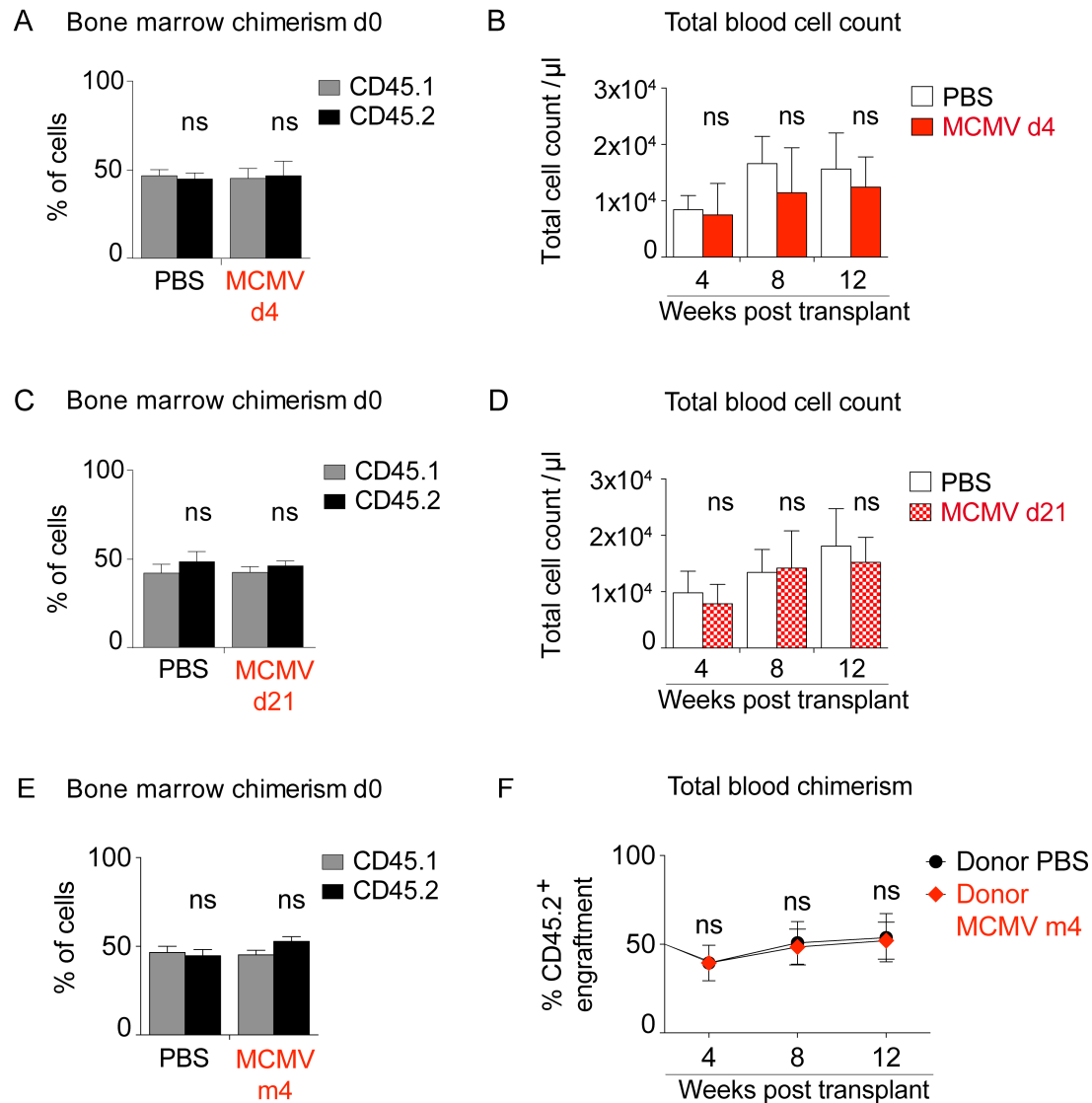


Figure S4 (related to Figure 4):

(A) Chimerism of bone marrow graft mixtures prior to transplantation, set up according to Fig. 6A (5×10^5 PFU MCMV, 4 dpi) ($n = 7-10$; $N = 2$). (B) Total blood cell count post transplantation of (A) ($n = 7-10$; $N = 2$). (C) Chimerism of bone marrow graft mixtures prior to transplantation, set up according to Fig. 6A (5×10^5 PFU MCMV, 21 dpi) ($n = 7-11$; $N = 2$). (D) Total blood cell count post transplantation of (C) ($n = 7-11$; $N = 2$). (E) Chimerism of bone marrow graft mixtures prior to transplantation (left panel), set up according to Fig. 6A from WT mice 4 months post MCMV infection (m4) ($n = 6-7$; $N = 2$). (F) Total blood chimerism post transplantation of (E) ($n = 6-7$; $N = 2$). Error bars indicate mean \pm SD, significance determined by two-sided t-test (*, $p \leq 0.05$; **, $p \leq 0.0025$; ***, $p \leq 0.0001$; ns = not significant; n = biological replicates; N = experimental repetitions).

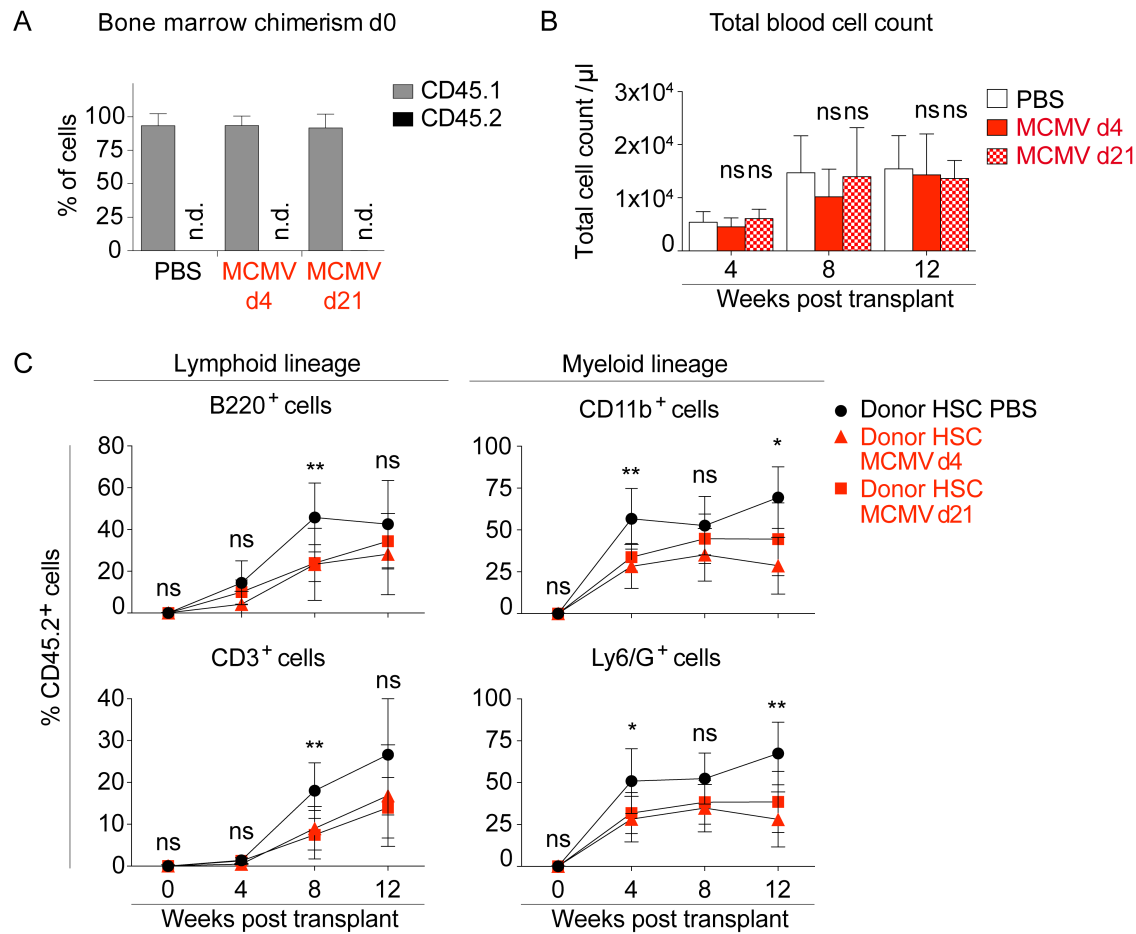


Figure S5 (related to Figure 5):

(A) Chimerism of bone marrow graft mixtures prior to transplantation, set up according to Fig. 6A (5×10^5 PFU MCMV 4 or 21 dpi) ($n = 7-14$; $N = 2$). (B) Total blood cell count post transplantation of (A) ($n = 7-10$; $N = 2$). (C) Contribution of CD45.2⁺ cells to lymphoid (B220⁺, CD3⁺) and myeloid (Ly6/G⁺, CD11b⁺) lineages post transplantation of (A) for mice showing engraftment of more than 5% CD45.2⁺ total blood cells at week 4 ($n = 5-9$; $N = 2$). Error bars indicate mean \pm SD, significance determined by two-sided t-test (*, $p \leq 0.05$; **, $p \leq 0.0025$; ***, $p \leq 0.0001$; ns = not significant; n = biological replicates; N = experimental repetitions).

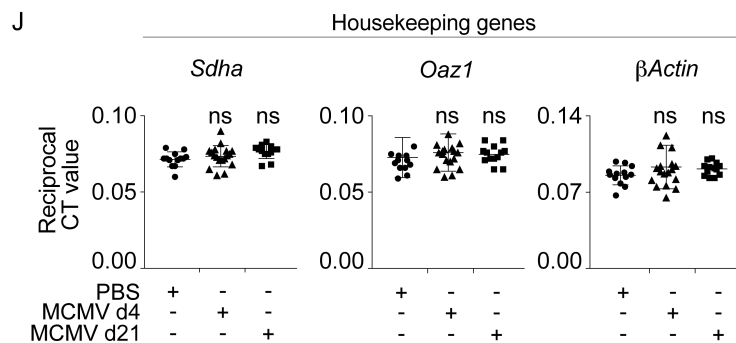
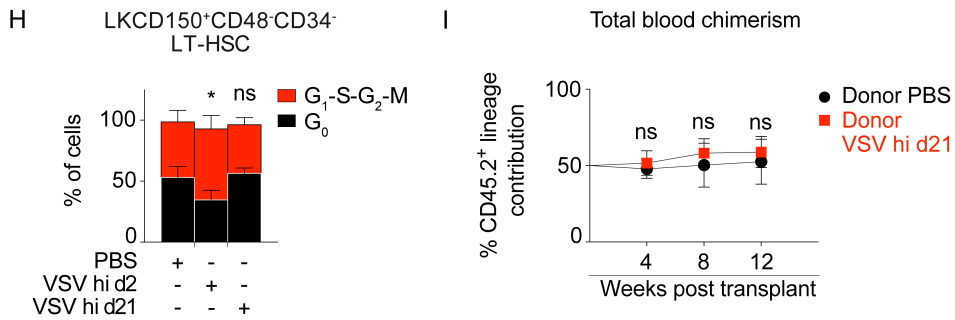
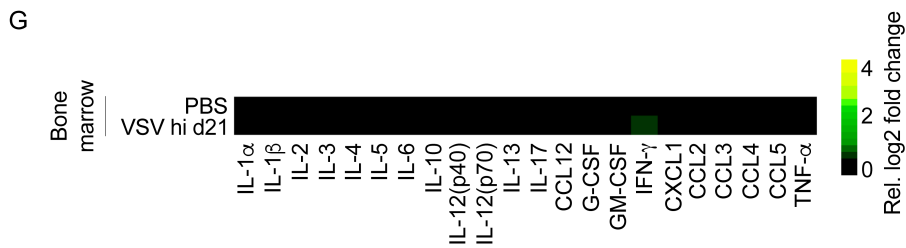
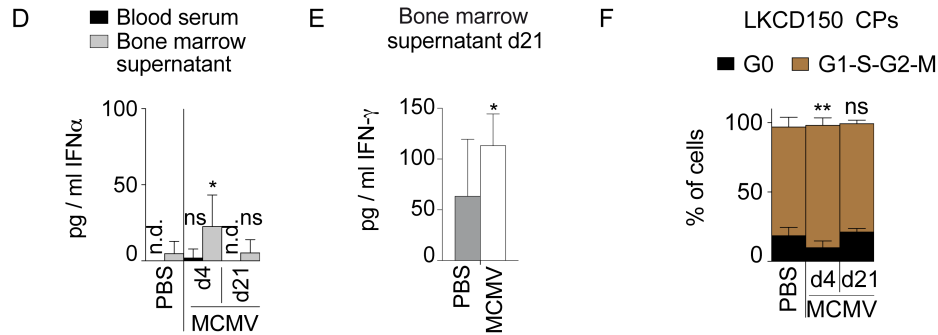
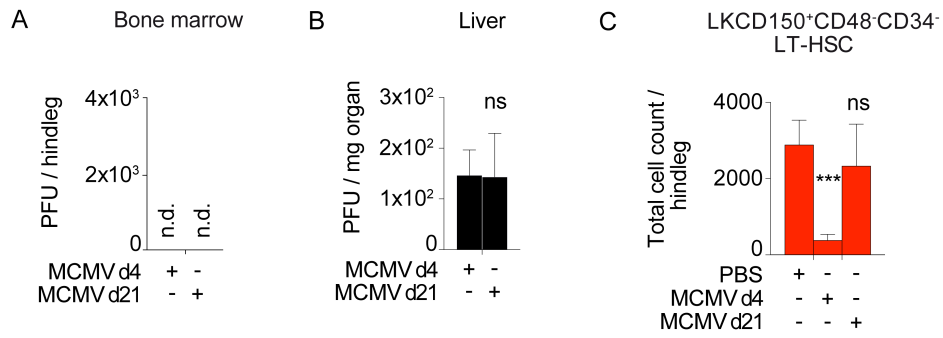


Figure S6 (related to Figure 6):

(A) Viral titers in bone marrow 4 and 21 dpi of WT mice infected i.v. with 5×10^5 PFU MCMV ($n = 6$; $N = 2$). **(B)** Viral titers in livers of MCMV-infected WT mice 4 and 21 dpi ($n = 6$; $N = 2$). **(C)** LT-HSC cell count of MCMV-infected WT mice 4 and 21 dpi ($n = 8-11$; $N = 3$). **(D)** IFN- α ELISA of blood sera and bone marrow supernatants of MCMV-infected WT mice 4 and 21 dpi ($n = 6-13$; $N = 2$). **(E)** IFN- γ ELISA of bone marrow supernatants of MCMV-infected WT mice 4 and 21 dpi ($n = 10$; $N = 2$). **(F)** Intracellular Ki-67/Hoechst staining for quiescent (G_0) and activated (G_1 -S- G_2 -M) committed progenitors (CPs) of MCMV-infected WT mice 4 and 21 dpi ($n = 6-12$; $N = 3$). **(G)** Heat map of multiplex array for 22 cytokines and chemokines in bone marrow supernatants of WT mice 2 and 21 dpi infected i.v. with 1×10^7 PFU VSV-M2 (VSV hi) ($n = 3$; $N = 1$). Data normalized to WT PBS controls. **(H)** Intracellular Ki-67 / Hoechst staining for quiescent (G_0) and activated (G_1 -S- G_2 -M) LT-HSCs of mice from (G) ($n = 6-8$; $N = 2$). **(I)** Total blood chimerism post competitive transplantation of WT total bone marrow 21 dpi VSV hi infection (chimeras set up according to Fig. 4A) ($n = 6-8$; $N = 2$). **(J)** Single-cell RT-qPCR for housekeeping genes to verify gene expression shown in Fig. 6F ($n = 13-18$; $N = 1$). Error bars indicate mean \pm SD, significance determined by two-sided t-test (*, $p \leq 0.05$; **, $p \leq 0.0025$; ***, $p \leq 0.0001$; ns = not significant; n = biological replicates; N = experimental repetitions).

Primer	Sequence
<i>Evi1_fw</i>	AGTTTTCCCGATCTGCAA
<i>Evi1_rev</i>	CCTTGGGACACTGATCACACT
<i>Scl_fw</i>	CAGCCTGATGCTAAGGCAAG
<i>Scl_rev</i>	AGCCAACCTACCATGCACAC
<i>Sca-1_fw</i>	TGGATTCTCAAACAAGGAAAGTAAAGA
<i>Sca-1_rev</i>	ACCCAGGATCTCCATACTTTCAATA
<i>Isg15_fw</i>	TCCTTAATTCCAGGGGACCTA
<i>Isg15_rev</i>	ACCGTCATGGAGTTAGTCACG
<i>Gbp6_fw</i>	CAGGAAGAAGGTTGAACAGGA
<i>Gbp6_rev</i>	GCTCTGAAGGACATGATTTGC
<i>MAT_fw</i>	CCAGCGCGGTTGGAGACGTC
<i>MAT_rev</i>	GACGGGCAGTCGGTCGGATG

Supplemental Table S1: Bulk and single cell qPCR primers (related to Figure 6):

Forward (fw) and reverse (rev) primers utilized in bulk and / or single cell qPCR analyses for respective genes.